Article

Not peer-reviewed version

Assessment of Thermal Influence on an Orthodontic System by Means of the Finite Element Method

Stelian-Mihai-Sever Petrescu , Mihai Popescu , Mihai Raul Popescu , Dragoș Laurențiu Popa * , Dumitru Ilie , Alina Duță , Laurențiu Daniel Răcilă , Daniela Doina Vintilă , Gabriel Buciu , Anne-Marie Rauten

Posted Date: 11 September 2024

doi: 10.20944/preprints202409.0865.v1

Keywords: cone beam computed tomography; dental structures; finite element method; orthodontics; temperature maps

Article

Assessment of Thermal Influence on an Orthodontic System by Means of the Finite Element Method

Stelian-Mihai-Sever Petrescu [1,†], Mihai Popescu [2,†], Mihai Raul Popescu [3,*], Dragoș Laurențiu Popa [4,*], Dumitru Ilie [4], Alina Duță [4], Laurențiu Daniel Răcilă [5], Daniela Doina Vintilă [5], Gabriel Buciu [6,†] and Anne-Marie Rauten [1]

[1] Department of Orthodontics, Faculty of Dental Medicine, University of Medicine and Pharmacy of Craiova, 200349 Craiova, Romania
[2] Department of Pedodontics, Faculty of Dental Medicine, University of Medicine and Pharmacy of Craiova, 200349 Craiova, Romania
[3] Department of Occlusology and Fixed Prosthetics, Faculty of Dental Medicine, University of Medicine and Pharmacy of Craiova, 200349 Craiova, Romania
[4] Department of Automotive, Transportation and Industrial Engineering, Faculty of Mechanics, University of Craiova, 200478 Craiova, Romania
[5] Department of Applied Mechanics, Faculty of Mechanics, University of Craiova, 200478 Craiova, Romania
[6] Department of General Nursing, Faculty of Nursing - Târgu Jiu, Titu Maiorescu University, 210102 Târgu Jiu, Romania
* Correspondence: popescumihairaul@yahoo.com (M.R.P.); popadragoslaurentiu@yahoo.com (D.L.P.)
† These authors contributed equally to this work.

Abstract: The development of the finite element method (FEM) combined block polynomial interpolation with the concepts of finite difference formats and the variation principle. Because of this combination, FEM overcomes the shortcomings of traditional variation methods while maintaining the benefits of current variation methods and the flexibility of the finite difference method. As a result, FEM is an advancement above the traditional variation methods. The aim of the study is to experimentally determine the thermal behavior of two stomatognathic systems, one control and the other presenting orthodontic treatment by means of a fixed metallic orthodontic appliance, both being subjected to several thermal regimes. In order to carry out this experimental study, we examined the case of a female subject, who was diagnosed with Angle class I malocclusion. The patient underwent a bimaxillary CBCT investigation before initiating the orthodontic treatment. A three-dimensional model with fully closed surfaces was obtained by using the InVesalius and Geomagic programs. Like the tissues examined in the patient, bracket and tube-like components, as well as orthodontic wires, can be included to these models. Once it is finished and geometrically accurate, the model is exported to a FEM-using program, such as Ansys Workbench. The intention was to study the behavior of two stomatognathic systems (with and without a fixed metallic orthodontic appliance) subjected to very hot food (70 ^{0}C) and very cold food (-18 ^{0}C). From the analysis of the obtained data, it was concluded that, following the simulations carried out in the presence of the fixed metallic orthodontic appliance, significantly higher temperatures were generated in the dental pulp.

Keywords: cone beam computed tomography; dental structures; finite element method; orthodontics; temperature maps

1. Introduction

Malocclusions are characterized by the impairment of the formation stages of the dento-maxillary apparatus. They have an ever-increasing prevalence as a result of environmental changes. Therefore, every etiopathogenic factor has a role in the more intricate modifications to the somatic development [1,2].

 doi:10.20944/preprints202409.0865.v1

CBCT is the most suggestive diagnostic imaging method that has appeared recently, being able to provide submillimeter resolutions images for diagnosis, of superior quality and with shorter scan times [3].

The applicability of this imaging examination in the oro-maxillo-facial region is due to numerous advantages, such as: low cost price, low dose of radiation to which the patient is exposed and the small size of the tomograph. At the same time, the disadvantages are few in number: low contrast in soft tissues, image noise and the presence of motion artifacts [4].

The development of the finite element method (FEM) combined block polynomial interpolation with the concepts of finite difference formats and the variation principle. Because of this combination, FEM overcomes the shortcomings of traditional variation methods while maintaining the benefits of current variation methods and the flexibility of the finite difference method. As a result, FEM is an advancement above the traditional variation methods [5,6].

The activity of three-dimensional modeling is a process, in general, iterative and involves several stages, including recognition of needs, definition of the problem, synthesis and analysis. A certain component or subsystem of an integrative system is conceptualized by the user, subjected to analysis, improved through the analysis procedure and remodeled. This process is repeated until the three-dimensional model is optimized by the system of constraints imposed by reality. Components and subsystems are synthesized within the global system in a similar way. Another stage is the evaluation, which consists in determining the degree of achievement of the conditions imposed within the specifications established in the defining the problem phase. In the last stage, the remodeling and geometric optimization is performed [7].

The objective of the study is to experimentally determine the thermal behavior of two stomatognathic systems, one control and the other presenting orthodontic treatment by means of a fixed metallic orthodontic appliance, both being subjected to several thermal regimes.

2. Materials and Methods

The present study was approved by the Ethics Committee of the University of Medicine and Pharmacy of Craiova, Romania (approval reference no. 127/09.04.2024), in accordance with the ethical guidelines for research with human participants of the University of Medicine and Pharmacy of Craiova, Romania. Written informed consent was obtained from the patient involved in the study.

In order to carry out this experimental study, we examined the case of a female subject, who presented herself in the Orthodontic Clinic of the Faculty of Dental Medicine of the University of Medicine and Pharmacy in Craiova, Romania.

After the orthodontic examination, the patient was diagnosed with Angle class I malocclusion, dento-alveolar disharmony with crowding. It was decided to apply a fixed metallic orthodontic appliance, using the straight-wire technique.

At the same time, for this research, the patient underwent a bimaxillary CBCT imaging investigation. A set of 586 tomographic images was used.

A Lenovo laptop computing system with the following technical characteristics was used: INTEL Core I5 processor with a frequency of 2.9 GHz; classic hard disk of 930 GB; RAM memory of 16 Gb; SSD hard disk of 476 GB; Windows 10 64-bit operating system.

The thermal simulations applied to the models, using the finite element method, the processing and organization of the obtained data, but also for the generation of virtual models, were obtained with a Hewlett Packard graphics station with the following main technical characteristics: processor-Intel® Core™ i9-13900K (up to 5.8 GHz with Intel® Turbo Boost Technology, 36 MB L3 cache, 24 cores); processor cache-L3 of 36 MB; family-13th generation Intel® Core™ i9 processor; memoryRAM MHz DDR5-4800 of 64 GB (4 x 16 GB); graphics-NVIDIA RTX™ A4500 (20 GB dedicated GDDR6 memory); graphics-Intel® UHD Graphics; memory and storage-64 GB memory/ TB SSD storage; memory Slots-4 DIMMs; internal Storage-SSD HP Z Turbo Drive PCIe® NVMe™ TLC of 1 TB; operating system-Windows 11 Pro.

InVesalius (CTI, Campinas, Brazil) is a free download program for the generation of three-dimensional geometric structures starting from sets of images obtained by computed tomography

 doi:10.20944/preprints202409.0865.v1

(CT or CBCT) or by magnetic resonance. The program is dedicated to research in the medical field which, based on the different shades of gray of the human body tissues, allows the obtaining of a primary geometry. This primary geometry consists of "clouds of points" and it is contained in stereolithography type files (obj, stl), similar to those obtained by three-dimensional scanning.

Geomagic (3D Systems, Rock Hill, SC, USA) is a program dedicated to Reverse Engineering that allows the processing of files that contain "clouds of points". It is known that the primary geometry of tissues contains so-called artifacts, i.e. virtual objects that do not exist in the human body, but which appear on tomographic images, due to the effects generated by the phenomena of refraction and reflection of X-rays. Also, this software allows the elimination of non-conforming surfaces, self-intersections surfaces, etc.

SolidWorks (Dassault Systèmes, Velizy-Villacoublay, France) is a computer-aided design (CAD) program that uses techniques and methods specific to Direct Engineering. This software allows the chaining of shapes to generate a virtual solid, but also the operation in environments specific to Multi Body models. For example, a perfectly closed surface generated in Geomagic is automatically transformed into a virtual solid in SolidWorks.

Ansys Workbench (Ansys, Inc., Canonsburg, PA, USA) is a software that allows the simulation of a multitude of physical phenomena applied to some virtual solid models and allows obtaining their physical behavior based on the result maps. This program operates with algorithms specific to the finite element method.

This program package (Microsoft Corporation, Redmond, Washington, USA) was used to organize and interpret the data obtained from the result maps given by the simulations in Ansys, but also to obtain some figures, graphs or diagrams.

For the development of thermal simulations, the following methods were used:

- Direct Engineering methods, included, in particular, in the SolidWorks program, which allow the generation of virtual objects similar to reality models, such as orthodontic arches or bracket-type elements;
- Reverse Engineering methods, which are the basis of the Geomagic program, used for editing and preparing models that, initially, were composed of the so-called "clouds of points";
- Thermodynamics methods that were used to define the simulations made in Ansys Workbench;
- Techniques specific to the finite element method that are the basis of the algorithms contained in the thermal modules of the Ansys program.

2.1. Elaboration of the Three-Dimensional Model of a Stomatognathic System Quasi-Identical to the Patient's

Initially, the set of CBCT tomographic images was loaded into the InVesalius program and the Enamel filter was used for the dental enamel. Figure 1 shows the interface of this program.

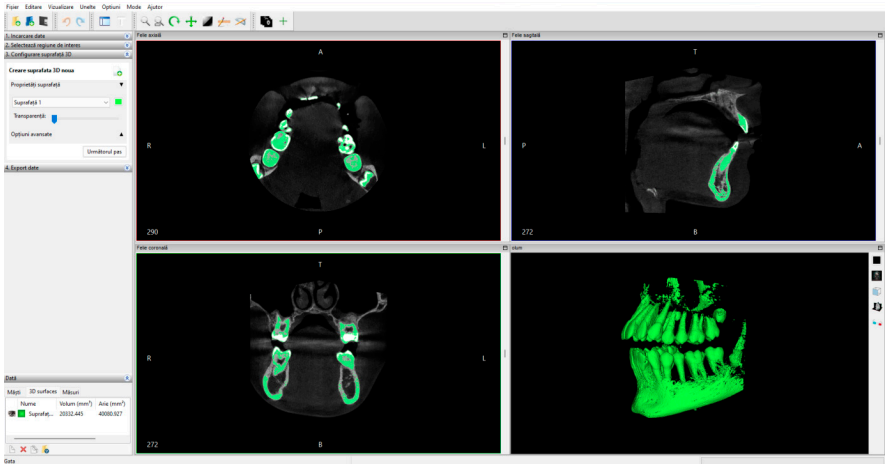

Figure 1. The interface of the InVesalius program with the Enamel filter activated.

 doi:10.20944/preprints202409.0865.v1

This primary "cloud of points" geometry was loaded into the Geomagic program for editing and processing, as it can be seen in Figure 2.

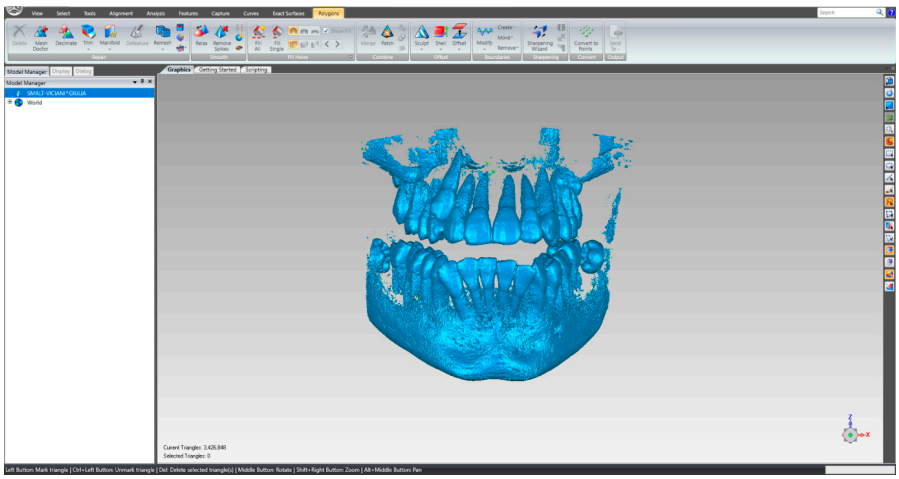

Figure 2. The primary geometry loaded in the Geomagic program.

Due to the similar density of the mandible and maxilla bones to the density of dental enamel, areas of these bones are found in this initial model. For this reason, these areas will be removed manually. Stages of these removal operations are shown in Figure 3.

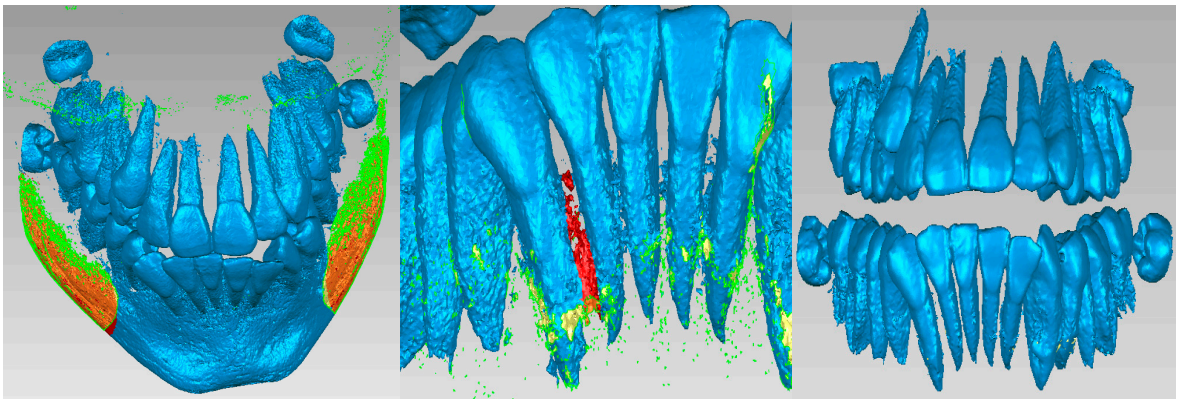

Figure 3. Steps to remove the bone components from the initial geometry in Geomagic.

Next, the wisdom teeth were removed, as it can be seen in Figure 4.

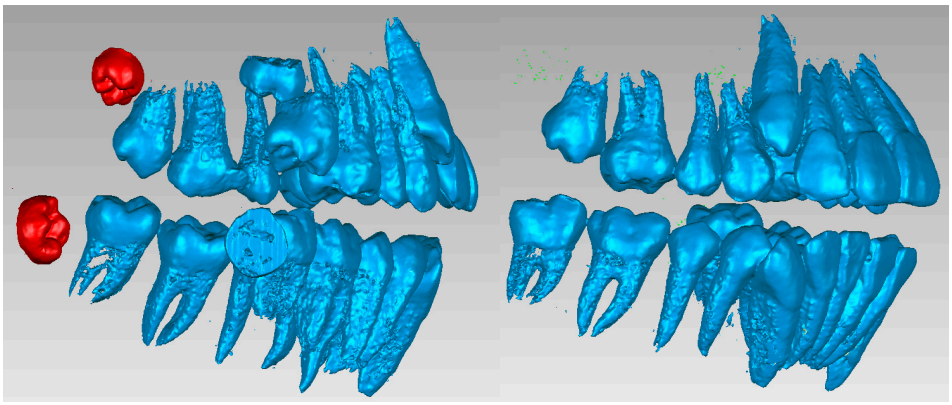

Figure 4. Removing the wisdom teeth from the dentition model.

Preprints.org (www.preprints.org) | NOT PEER-REVIEWED | Posted: 11 September 2024 doi:10.20944/preprints202409.0865.v1

Next, the model was subjected to operations to eliminate non-conforming surfaces, but also to other techniques to reduce the number of surfaces, etc. Figure 5 shows the final model of the dentition in Geomagic, then in SolidWorks.

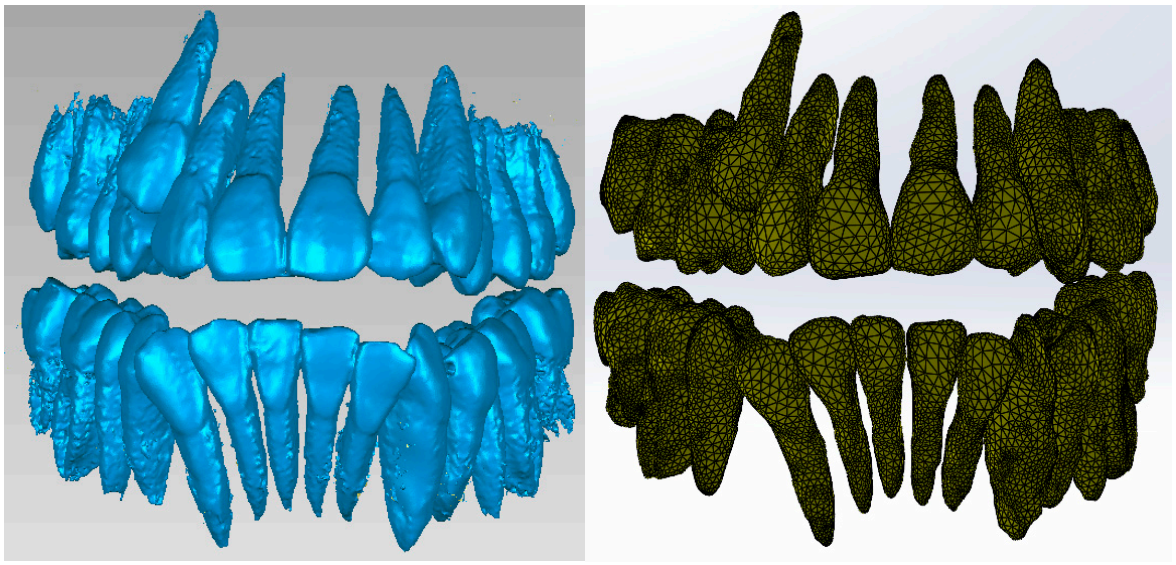

Figure 5. The final model of the dentition in Geomagic and SolidWorks.

To obtain the three-dimensional model of the bone components, the CBCT tomographic image set was loaded into the InVesalius program and the Compact Bone filter was activated, as it can be seen in Figure 6.

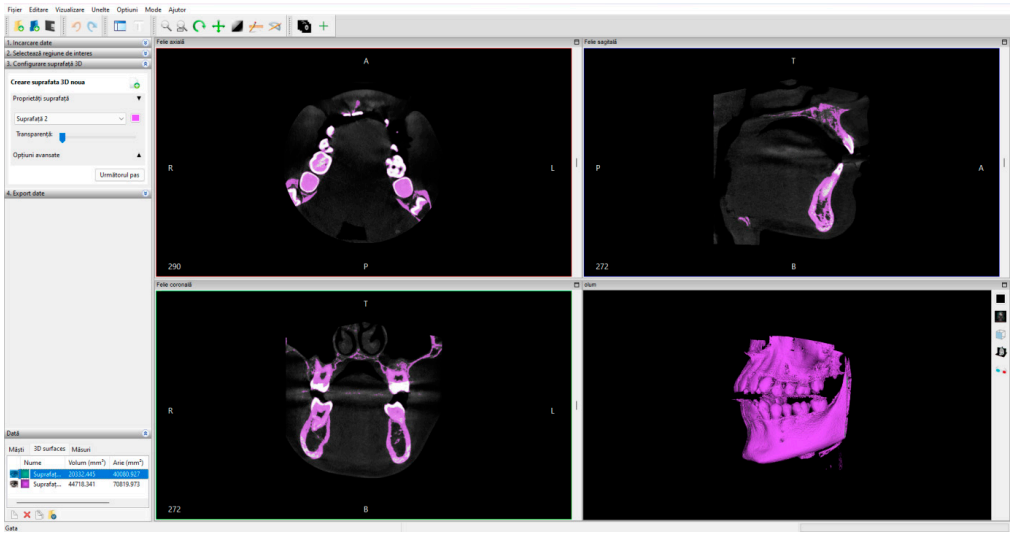

Figure 6. The interface of the InVesalius program with the Compact Bone filter activated.

Due to the fact that the bone density is relatively similar to tooth enamel density, it is necessary to remove these dental structures. Figure 7 shows these removal operations.

 doi:10.20944/preprints202409.0865.v1

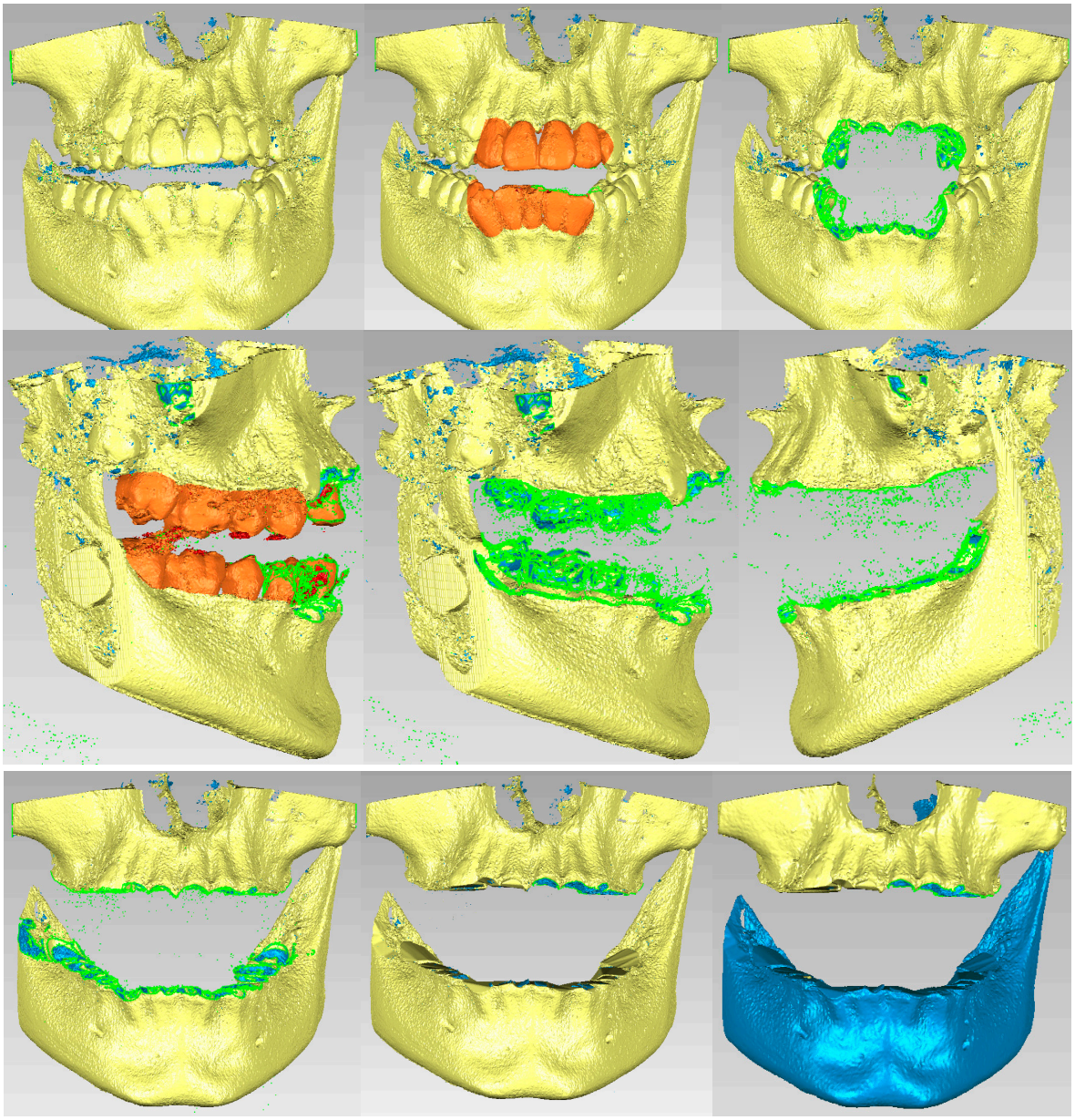

Figure 7. Processing stages of the model in Geomagic.

Next, specific Reverse Engineering techniques were applied and the final model of the bone components was obtained. Figure 8 shows the final model in Geomagic and SolidWorks.

 doi:10.20944/preprints202409.0865.v1

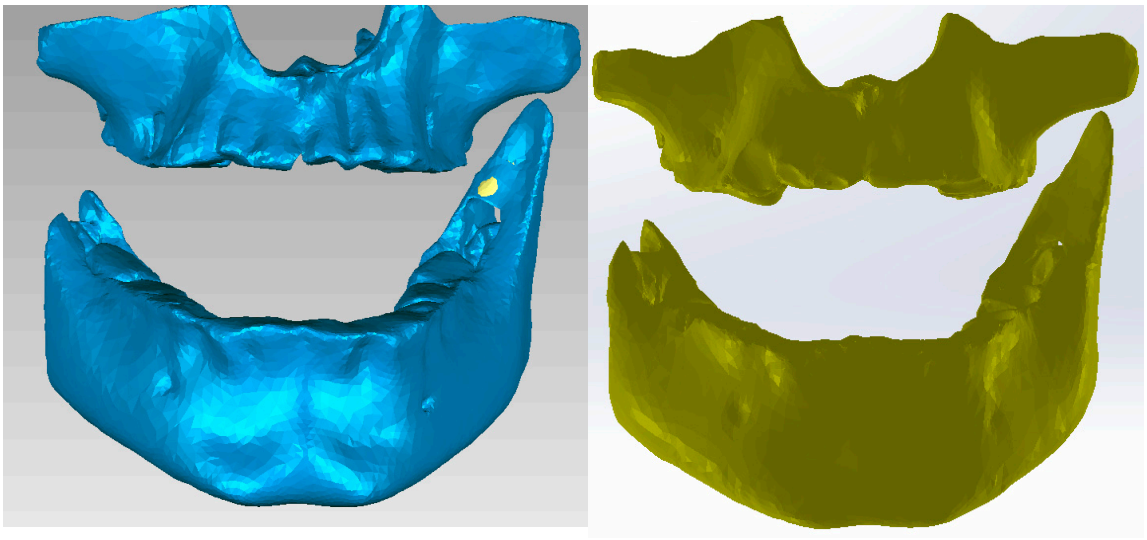

Figure 8. The virtual model of the bone components in Geomagic and in SolidWorks.

Using Direct Engineering known techniques and methods, the model of the patient's stomatognathic apparatus was obtained, as it can be seen in Figure 9. When aligning the models, the unique coordinate system was used, which is the same, because the models come from the same CBCT set.

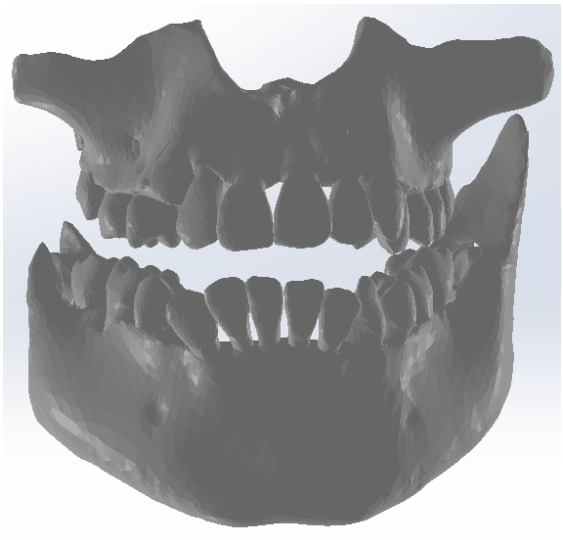

Figure 9. The virtual model of the studied stomatognathic apparatus.

To obtain the internal structures of teeth 1.1 and 4.1, initially, the dental enamel models for the two teeth were isolated in Geomagic, as it can be seen in Figure 10.

 doi:10.20944/preprints202409.0865.v1

Figure 10. Dental enamel models of teeth 1.1 and 4.1.

Next, tooth 1.1 was isolated, as it can be seen in Figure 11.

Figure 11. The external model of tooth 1.1 in Geomagic.

Then, Offset techniques were applied on the entire model or on some areas of the model to obtain the outer model of the dentin. These operations are shown in Figure 12.

Preprints.org (www.preprints.org) | NOT PEER-REVIEWED | Posted: 11 September 2024 doi:10.20944/preprints202409.0865.v1

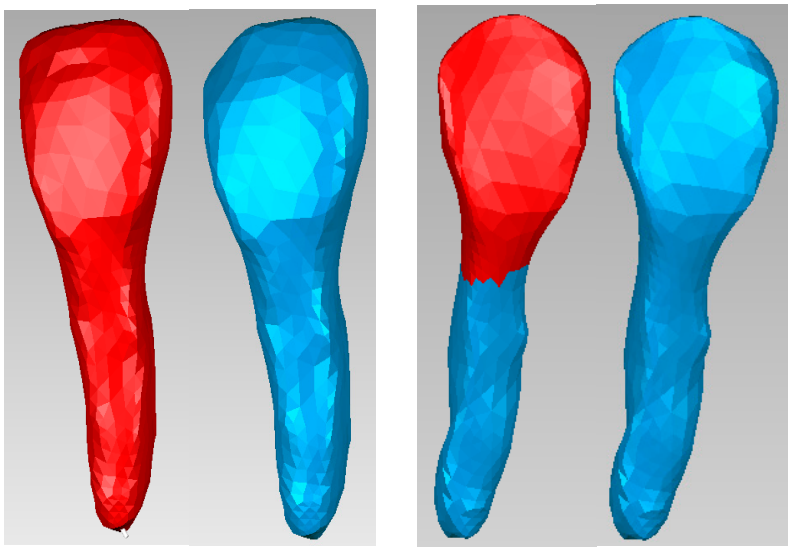

Figure 12. Obtaining the dentine model of tooth 1.1.

Starting from the dentine model, applying similar Offset techniques, the model of tooth 1.1 pulp was finally obtained. Figure 13 shows the final model of tooth 1.1 pulp in Geomagic and SolidWorks.

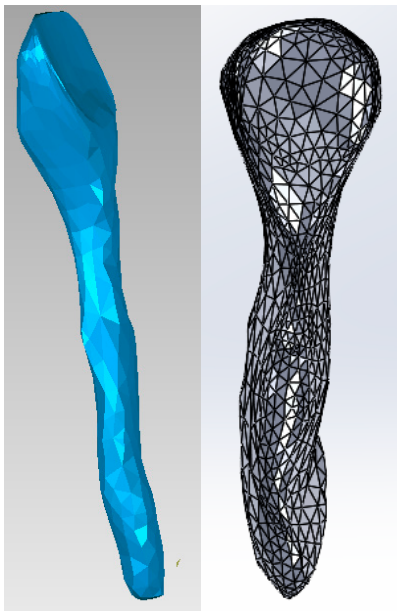

Figure 13. Model of the dental pulp of tooth 1.1 in Geomagic and SolidWorks.

The same procedure was used to obtain the dentine and pulp models for tooth 4.1. Figure 14 shows these models.

 doi:10.20944/preprints202409.0865.v1

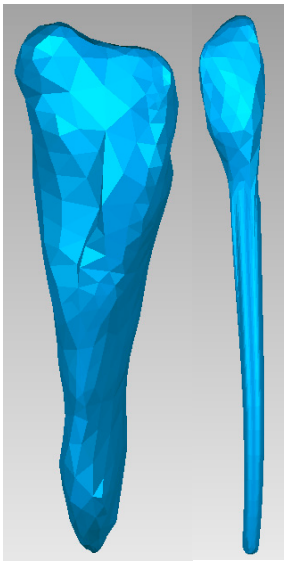

Figure 14. The dentin and dental pulp models of tooth 4.1.

These models representing the enamel, dentin and pulp of teeth 1.1 and 4.1 were loaded into the Assembly module of SolidWorks, and based on the coordinate systems, the models were aligned. Using volumetric reduction techniques, the final models of teeth 1.1 and 4.1 were obtained, as shown in Figure 15.

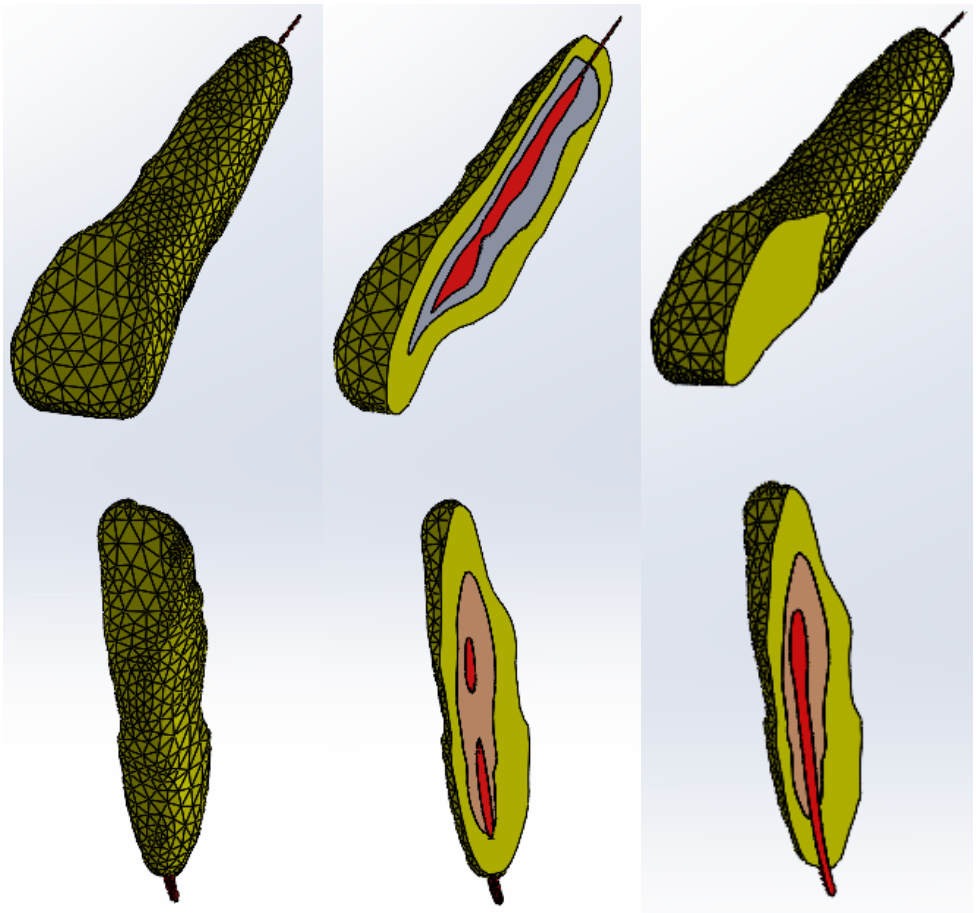

Figure 15. Final models of teeth 1.1 and 4.1 (one view and two sections).

Using Direct Engineering techniques and methods, the bracket and tube-type elements were modeled. Figure 16 shows four of these components.

Preprints.org (www.preprints.org) | NOT PEER-REVIEWED | Posted: 11 September 2024 doi:10.20944/preprints202409.0865.v1

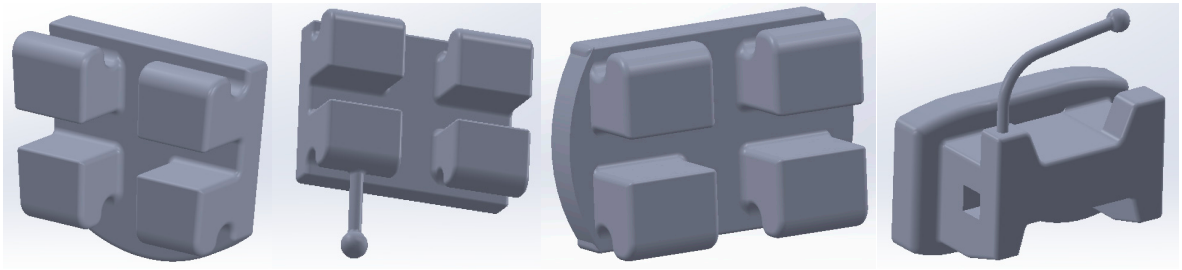

Figure 16. Bracket and tube-type elements.

These components were placed on the teeth according to orthodontic protocols. On each of these components, four points have been defined that will be found on the curves that define the orthodontic arches. Initially, two curves were drawn that "connected" these points that were placed above the bracket and tube-type elements, in close proximity. Later, using circular sections placed perpendicular to the curves, Sweep type shapes were defined that defined the orthodontic arches. Figure 17 shows these orthodontic arches placed on the dentition.

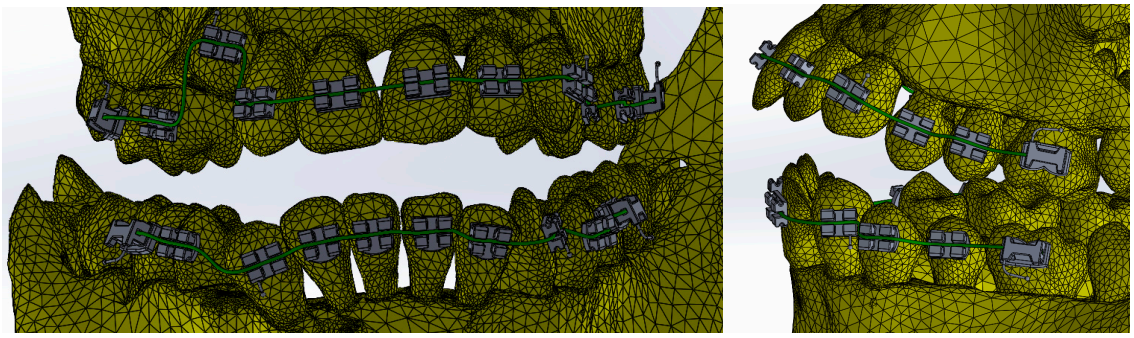

Figure 17. Placement of virtual orthodontic wires.

In Figure 18, sections through teeth 1.1 and 4.1 are shown.

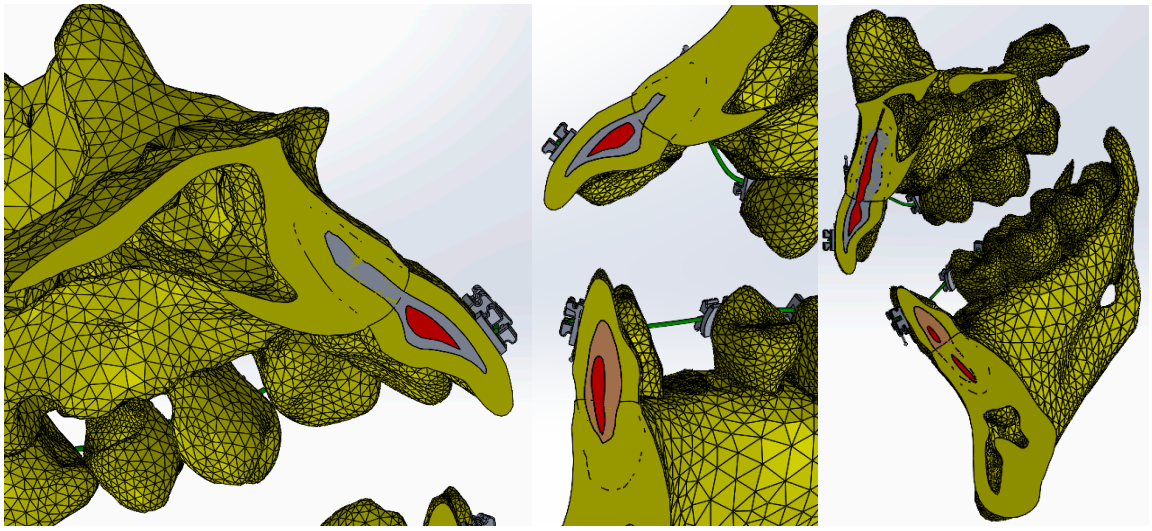

Figure 18. Sections through the studied orthodontic system.

2.2. Preparation of Thermal Simulations

Two groups of simulations were carried out for:

- The model of the control stomatognathic apparatus (in the obtained model, the bracket and tube-type elements and the orthodontic arches were suppressed);

 doi:10.20944/preprints202409.0865.v1

- The model of the stomatognathic apparatus with a fixed metallic orthodontic appliance.

These models were imported into Ansys Workbench, in the Transient Thermal module, where they were divided into finite elements. Figure 19 shows the finite element structure composed of 1,248,243 nodes and 726,343 elements for the model without a fixed metallic orthodontic appliance.

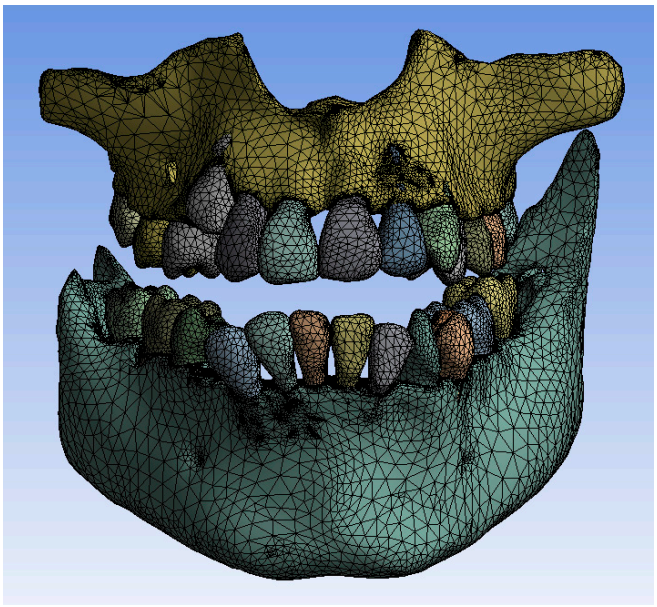

Figure 19. Finite element structure for simulations without a fixed metallic appliance.

Figure 20 shows the finite element structure composed of 1,489,889 nodes and 827,771 elements for the model with a fixed metallic orthodontic appliance.

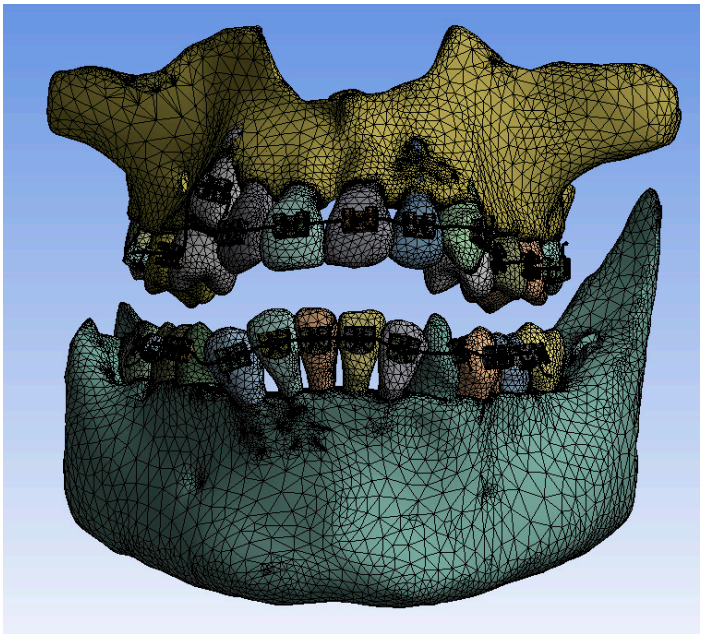

Figure 20. Finite element structure for simulations with a fixed metallic orthodontic appliance.

In the Engineering Data module, the materials used in the simulations were defined based on their physical and thermal properties. Table 1 shows these materials that were used. Obviously, for the simulations without a fixed metallic orthodontic appliance., the two alloys (Ni+Cr, Ni+Ti) were not used [8–16].

 doi:10.20944/preprints202409.0865.v1

Table 1. The thermal physical properties of the materials used in the simulations.

Component	Density [Kg/m³]	Isotropic Thermal Conductivity [W˙m/C⁰]	Specific Heat [J˙Kg/ C⁰]
Dental enamel	2958	0.93	710
Dentine	2140	0.36	1302
Pulp	1000	0.0418	4200
Mandible, maxillary	2310	1	2650
Bracket type components, Ni+Cr alloy	8500	13	460
Orthodontic arch, Ni+Ti alloy	6450	60	457

Next, a temperature source materialized by the surfaces that come into contact with hot or cold food was defined, as shown in Figure 21.

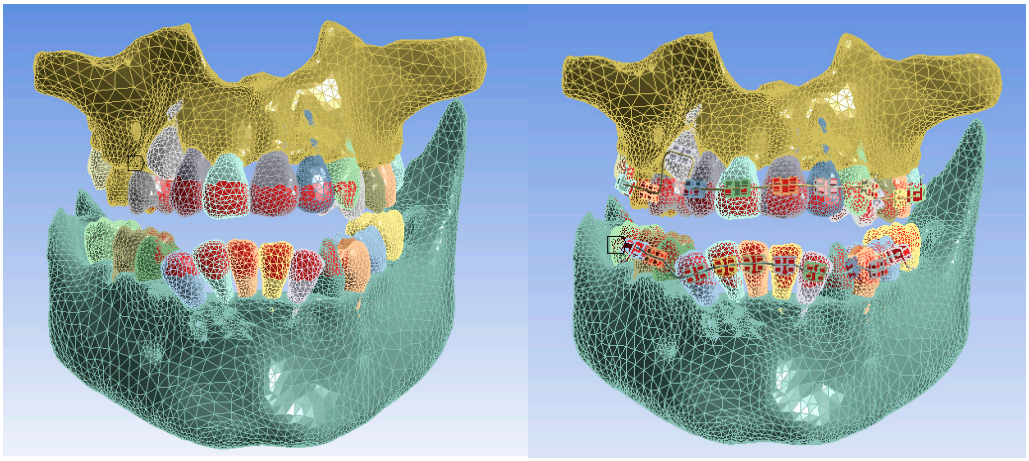

Figure 21. The areas in the models that come into contact with hot or cold food (temperature source).

It was intended to study the behavior of these two systems in different situations materialized in two situations:

- very hot food (70 ⁰C) that acts for 3 seconds, then the temperature tends to 37 ⁰C, and the cycle is repeated two more times, the whole regime lasts 20 seconds (Figure 22);

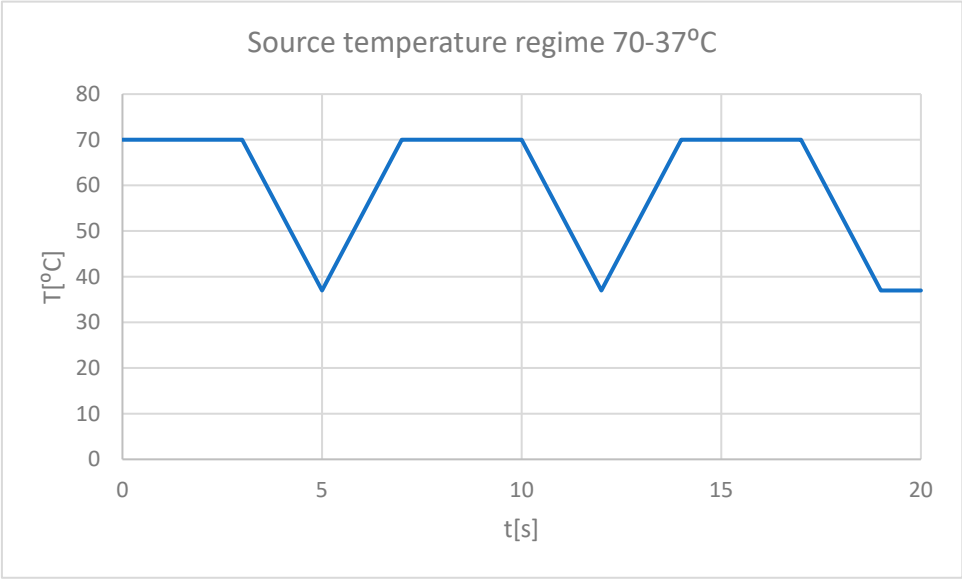

Preprints.org (www.preprints.org) | NOT PEER-REVIEWED | Posted: 11 September 2024 doi:10.20944/preprints202409.0865.v1

Figure 22. Mode of the heat source (hot food).

- very cold food (-18 ^{0}C) that acts for 3 seconds, then the temperature tends to 37 ^{0}C, and the cycle is repeated two more times, the whole regime lasts 20 seconds (Figure 23);

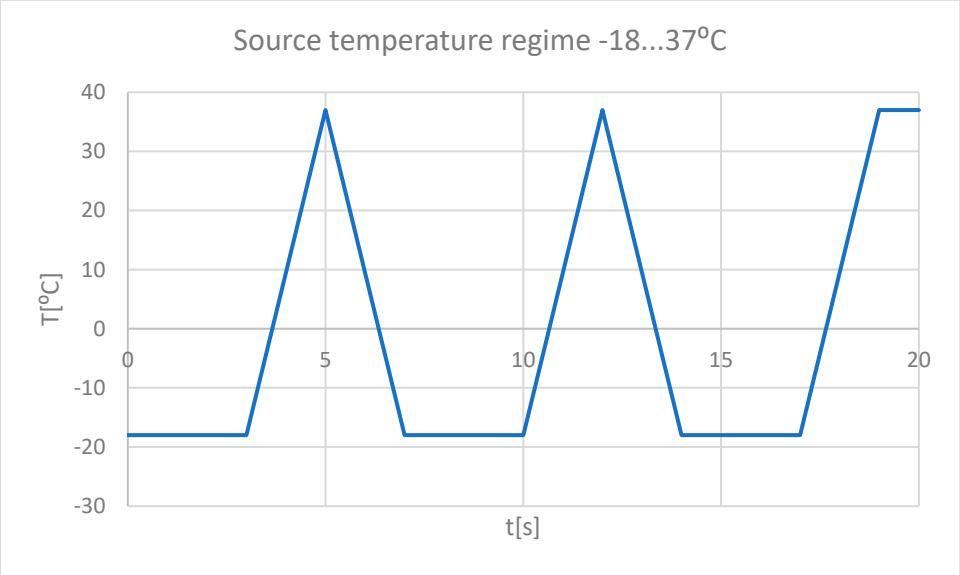

Figure 23. Heat source mode (cold food).

Next, the area where the convection phenomenon acts was defined, as it can be seen in Figure 24. The value of convection in the oral cavity is in the range of 2...3 W/m2 [17].

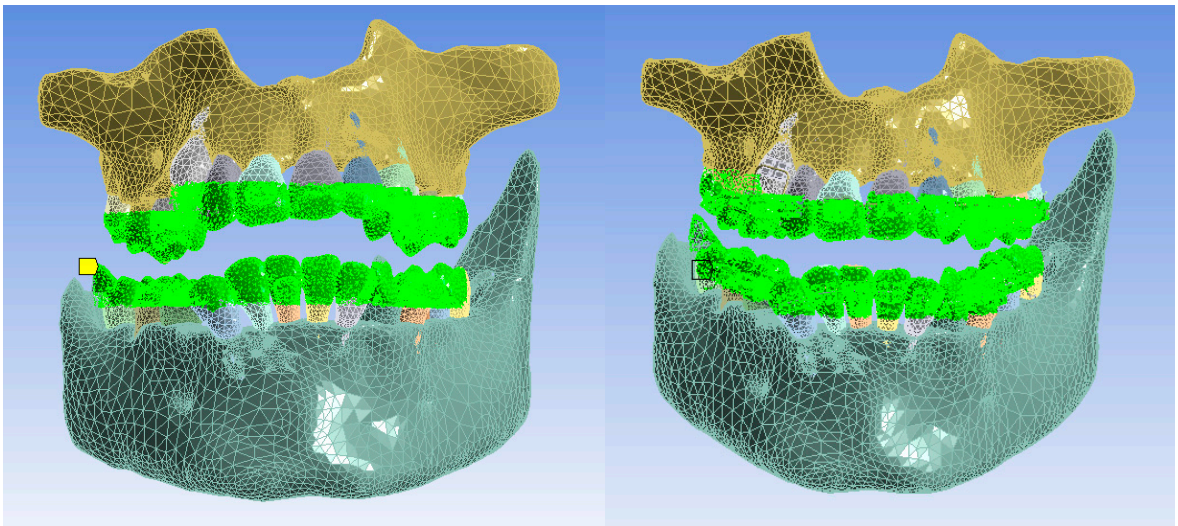

Figure 24. The areas where the phenomenon of thermal convection is present.

In order to determine the dynamic temperature on the structures of teeth 1.1 and 4.1, some virtual temperature sensors were placed on them (using the Probe command). They record the temperature vs. time, the values being taken in a Microsoft Excel type file.

3. Results

3.1. Thermal Simulation Results for the Stomatognathic Control System with a Hot Temperature Source

Figure 25 shows the temperature map of the system subjected to thermal simulation.

Preprints.org (www.preprints.org) | NOT PEER-REVIEWED | Posted: 11 September 2024 doi:10.20944/preprints202409.0865.v1

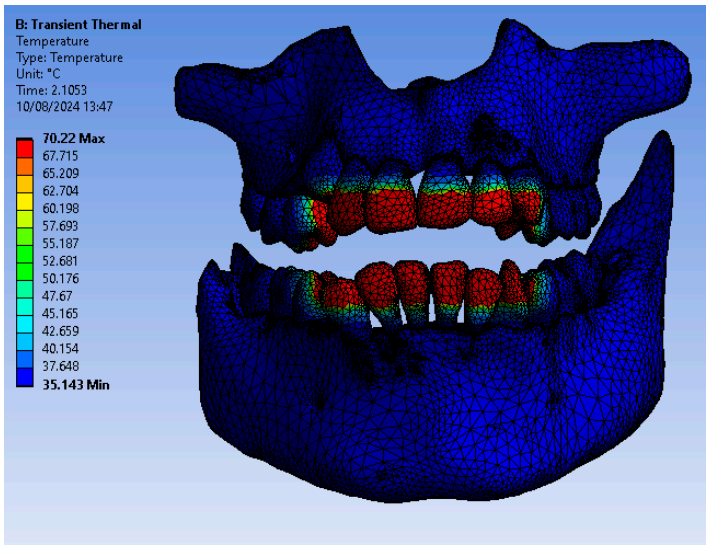

Figure 25. Temperature map.

Using the Probe-type virtual temperature sensors, the temperature diagram of the dental enamel (Figure 26), of the dentine (Figure 27), of the pulp (Figure 28) was obtained for tooth 1.1, the comparative diagram of the dental structures was obtained for tooth 1.1 (Figure 29), the temperature diagram of the dental enamel (Figure 30), of the dentine (Figure 31), of the pulp (Figure 32) was obtained for tooth 4.1, the comparative diagram of the dental structures was obtained for tooth 4.1 (Figure 33) and the comparative diagram of the dental structures was obtained for teeth 1.1, 4.1 (Figure 34).

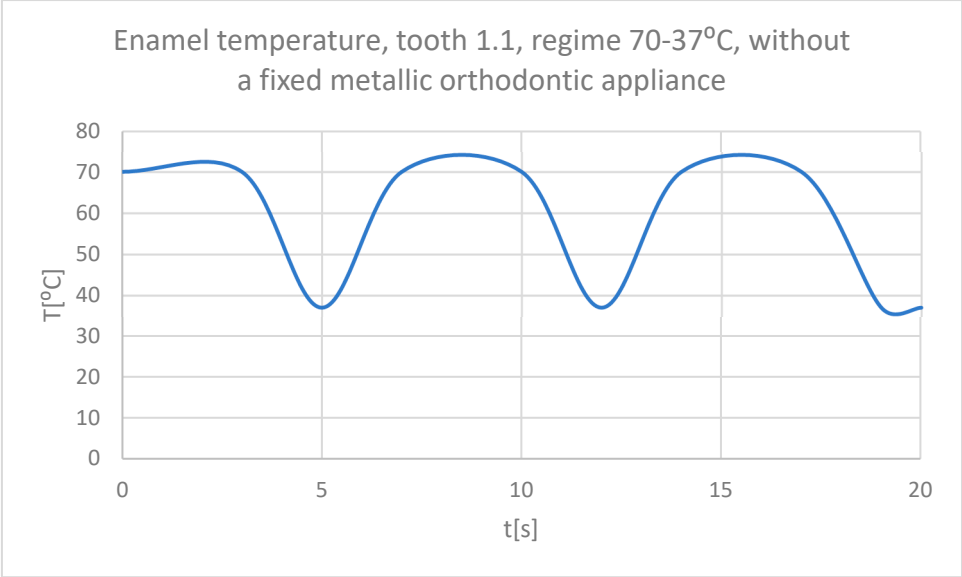

Figure 26. The temperature in the dental enamel of tooth 1.1 subjected to the hot thermal source.

Preprints.org (www.preprints.org) | NOT PEER-REVIEWED | Posted: 11 September 2024 doi:10.20944/preprints202409.0865.v1

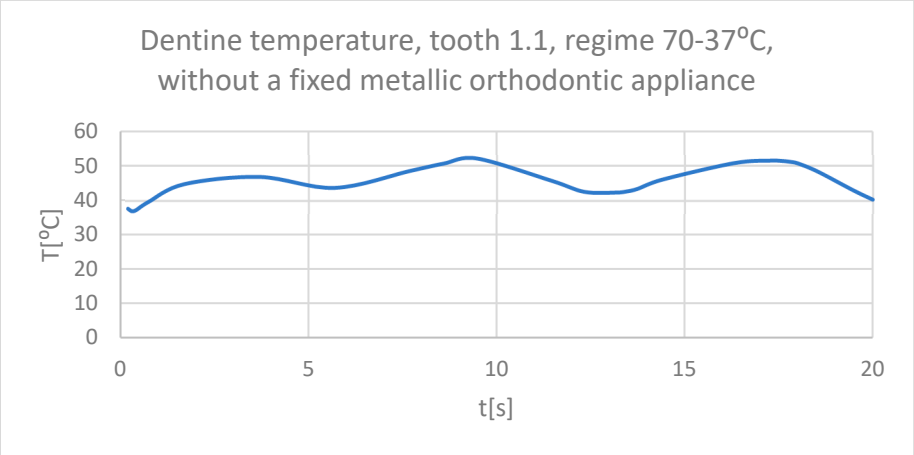

Figure 27. The temperature in the dentine of tooth 1.1 subjected to the hot thermal source.

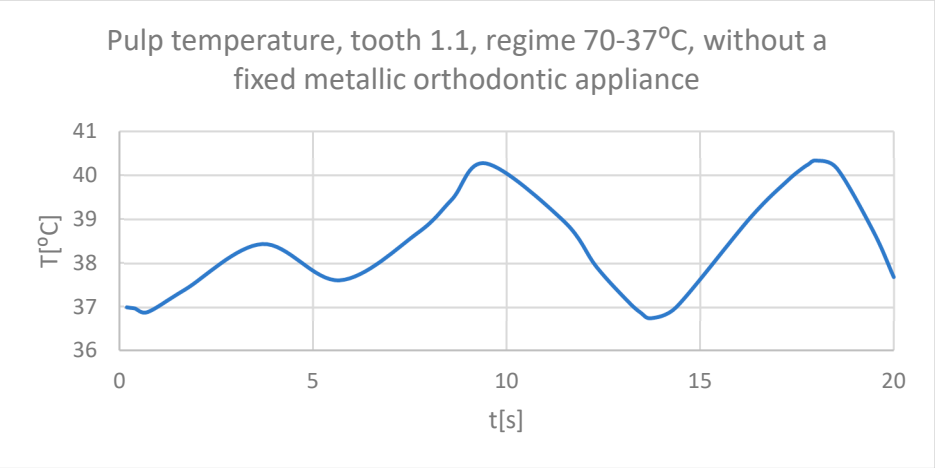

Figure 28. The temperature in the pulp of tooth 1.1 subjected to the hot thermal source.

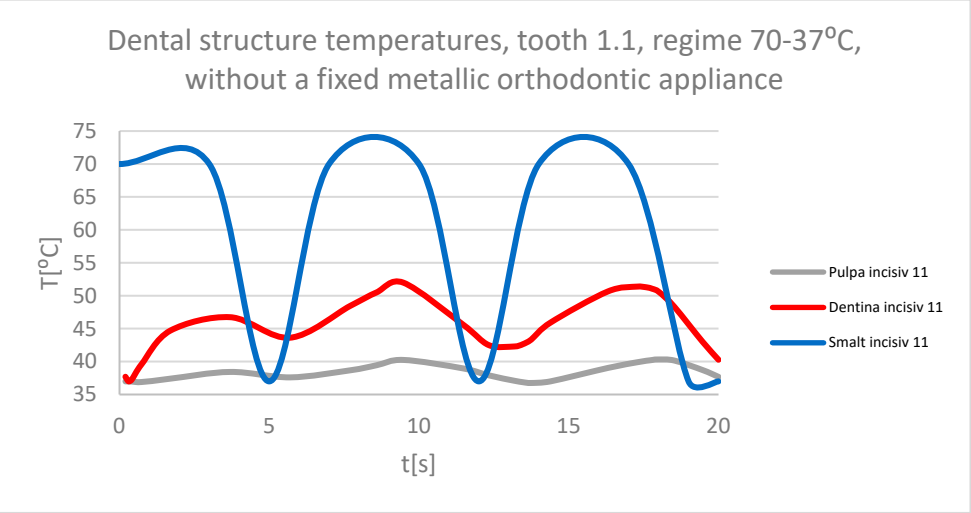

Figure 29. Comparative diagram of the dental structures temperatures of tooth 1.1 subjected to the hot thermal source.

Preprints.org (www.preprints.org) | NOT PEER-REVIEWED | Posted: 11 September 2024 doi:10.20944/preprints202409.0865.v1

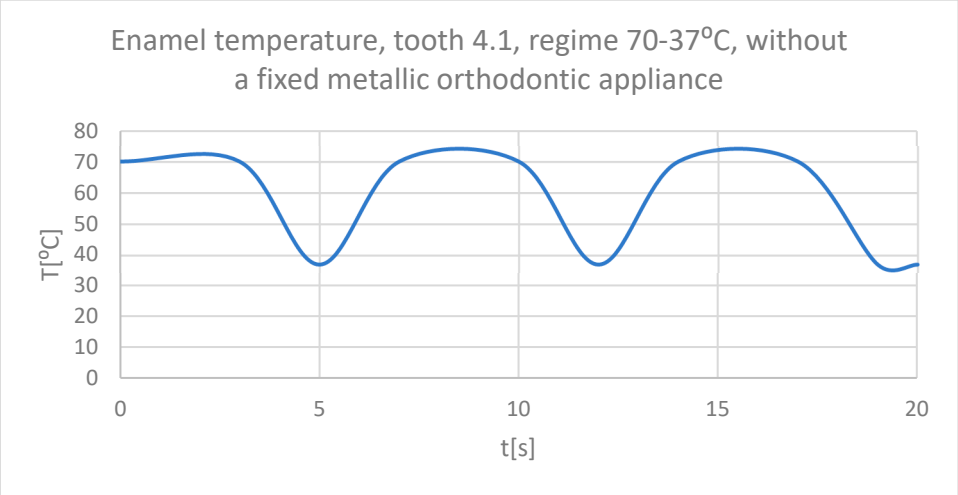

Figure 30. The temperature in the dental enamel of tooth 4.1 subjected to the hot thermal source.

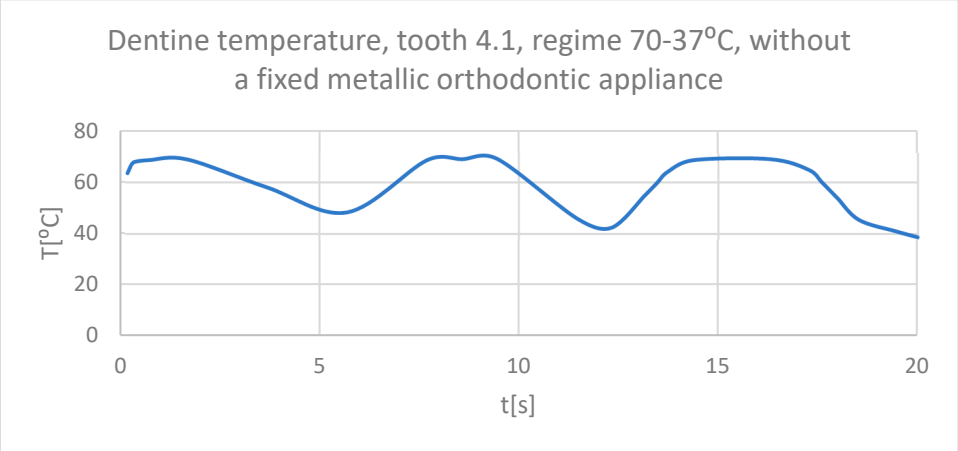

Figure 31. The temperature in the dentin of tooth 4.1 subjected to the hot thermal source.

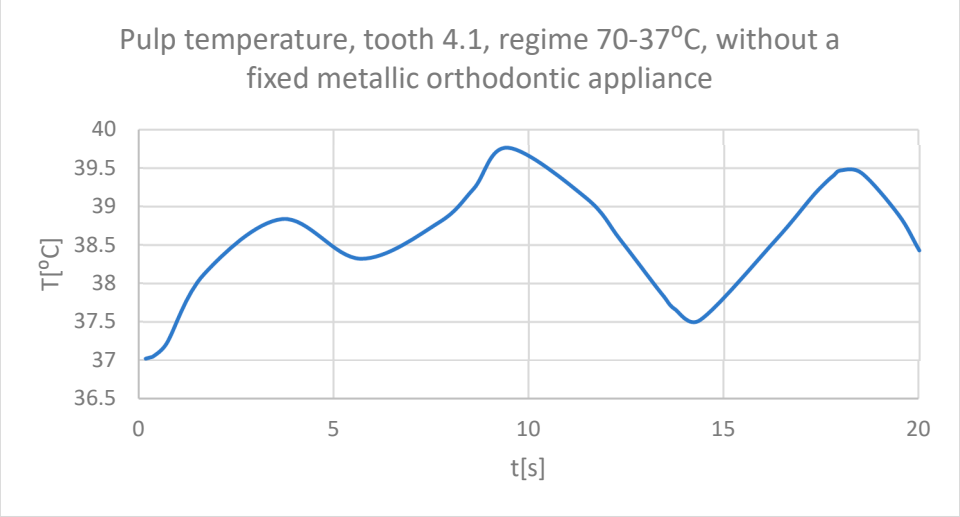

Figure 32. The temperature in the pulp of tooth 4.1 subjected to the hot thermal source.

 doi:10.20944/preprints202409.0865.v1

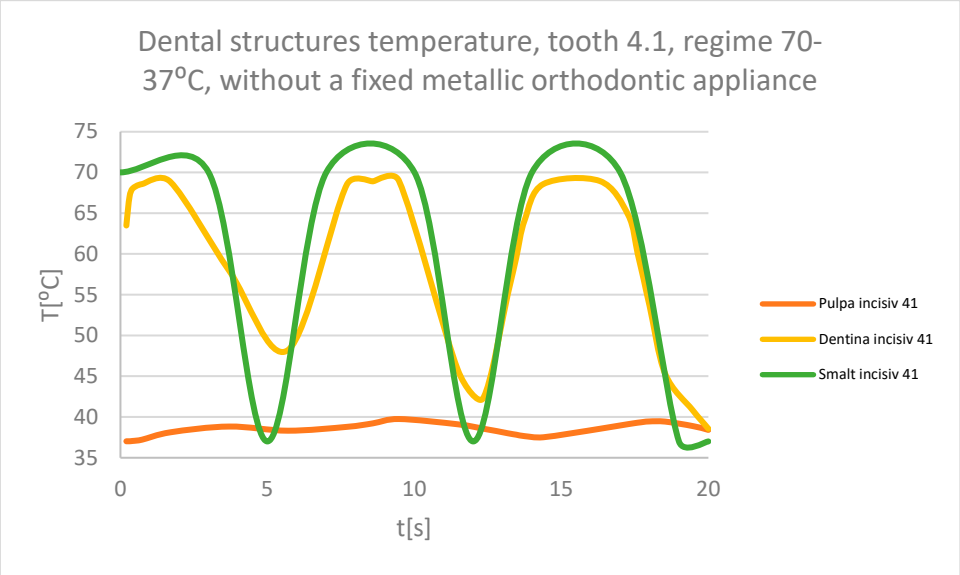

Figure 33. Comparative diagram of the dental structures temperatures of tooth 4.1 subjected to the hot thermal source.

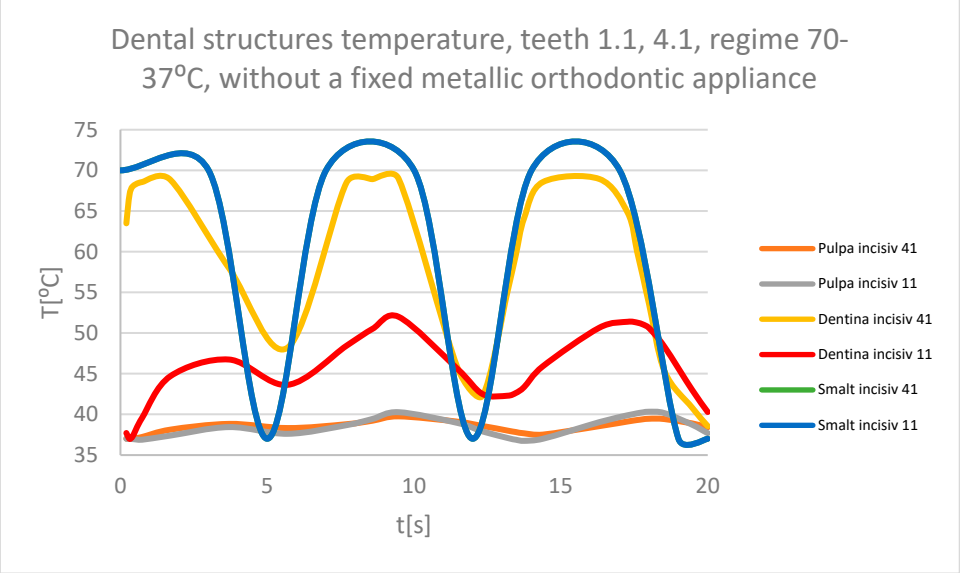

Figure 34. Comparative diagram of the dental structures temperatures of teeth 1.1, 4.1 subjected to the hot thermal source.

3.2. Thermal Simulation Results for the Stomatognathic Control System with a Cold Temperature Source

Figure 35 shows the temperature map of the system subjected to thermal simulation.

Preprints.org (www.preprints.org) | NOT PEER-REVIEWED | Posted: 11 September 2024 doi:10.20944/preprints202409.0865.v1

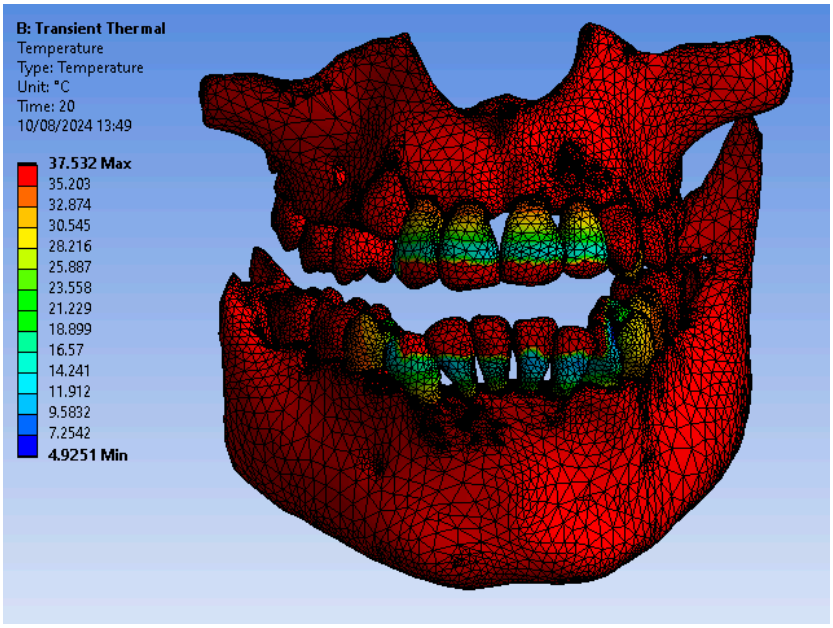

Figure 35. Temperature map.

Using the Probe-type virtual temperature sensors, the temperature diagram of the tooth enamel (Figure 36), of the dentine (Figure 37), of the pulp (Figure 38) was obtained for tooth 1.1, the comparative diagram of the dental structures was obtained for tooth 1.1 (Figure 39), the temperature diagram of the dental enamel (Figure 40), of the dentine (Figure 41), of the pulp (Figure 42) was obtained for tooth 4.1, the comparative diagram of the dental structures was obtained for tooth 4.1 (Figure 43) and the comparative diagram of the dental structures was obtained for teeth 1.1, 4.1 (Figure 44).

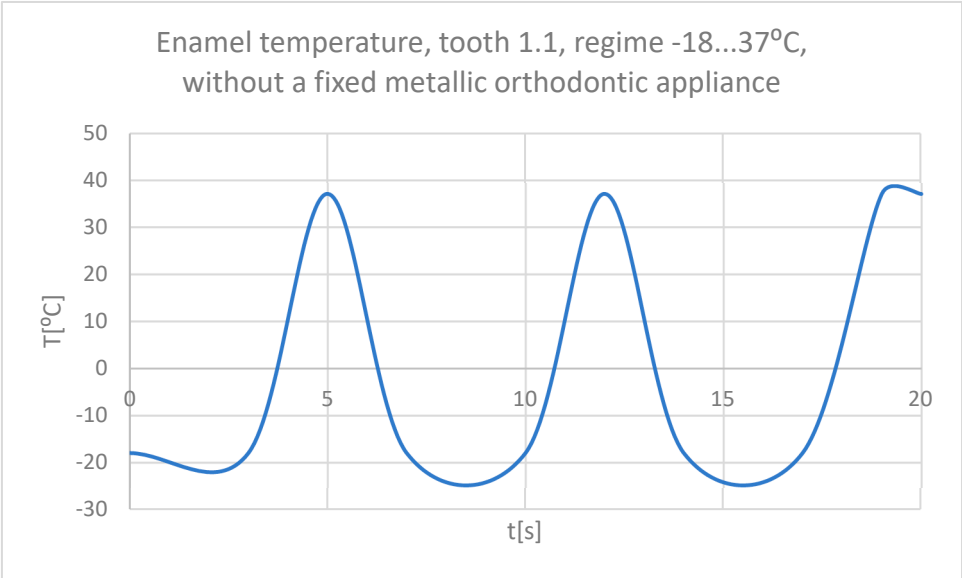

Figure 36. The temperature in the dental enamel of tooth 1.1 subjected to the cold thermal source.

Preprints.org (www.preprints.org) | NOT PEER-REVIEWED | Posted: 11 September 2024 doi:10.20944/preprints202409.0865.v1

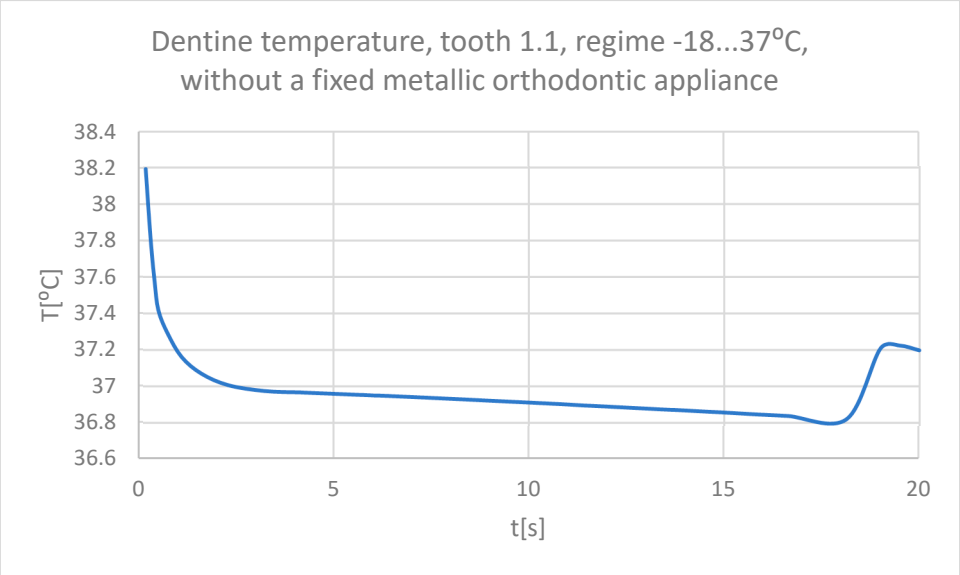

Figure 37. The temperature in the dentine of tooth 1.1 subjected to the cold thermal source.

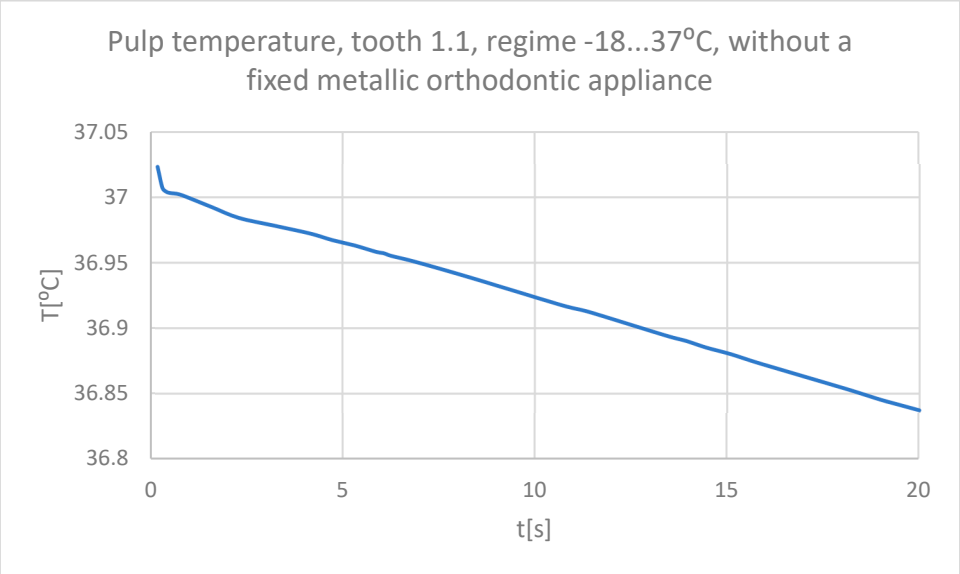

Figure 38. The temperature in the pulp of tooth 1.1 subjected to the cold thermal source.

Preprints.org (www.preprints.org) | NOT PEER-REVIEWED | Posted: 11 September 2024 doi:10.20944/preprints202409.0865.v1

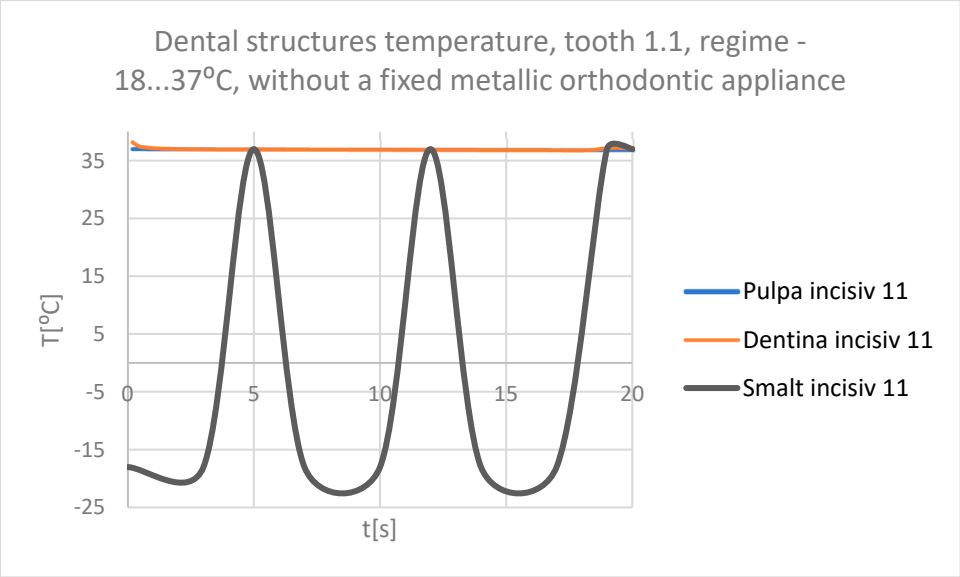

Figure 39. Comparative diagram of the dental structures temperatures of tooth 1.1 subjected to the cold thermal source.

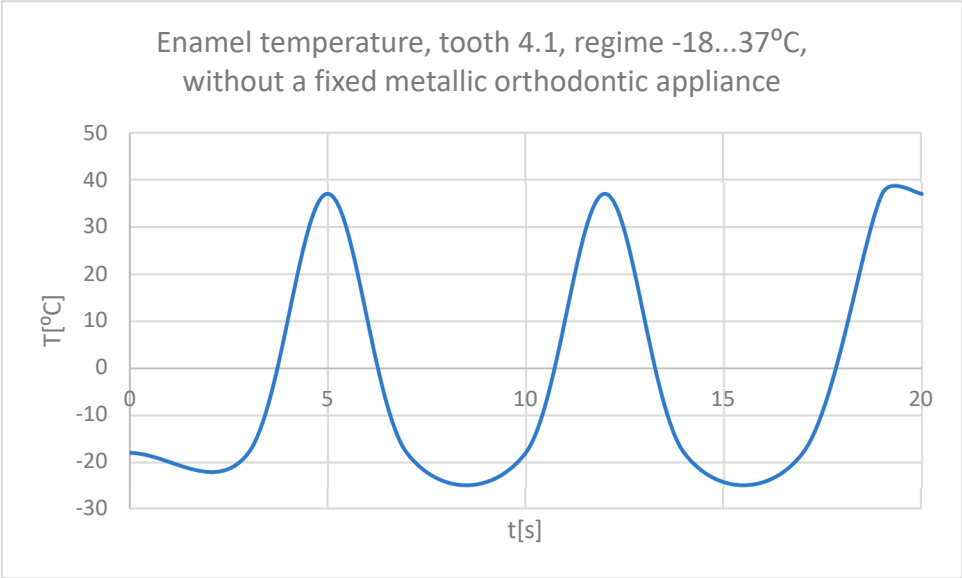

Figure 40. The temperature in the dental enamel of tooth 4.1 subjected to the cold thermal source.

Preprints.org (www.preprints.org) | NOT PEER-REVIEWED | Posted: 11 September 2024 doi:10.20944/preprints202409.0865.v1

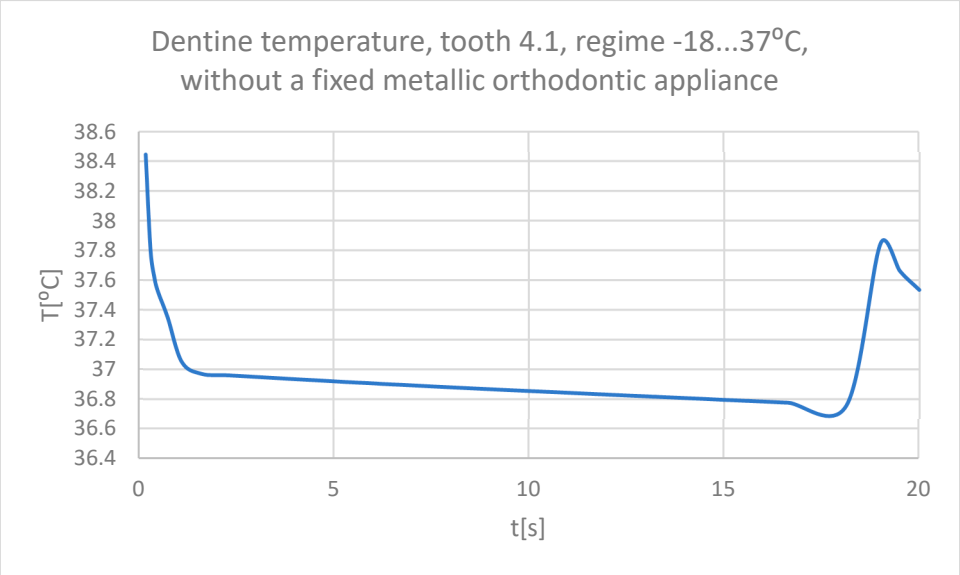

Figure 41. The temperature in the dentin of tooth 4.1 subjected to the cold thermal source.

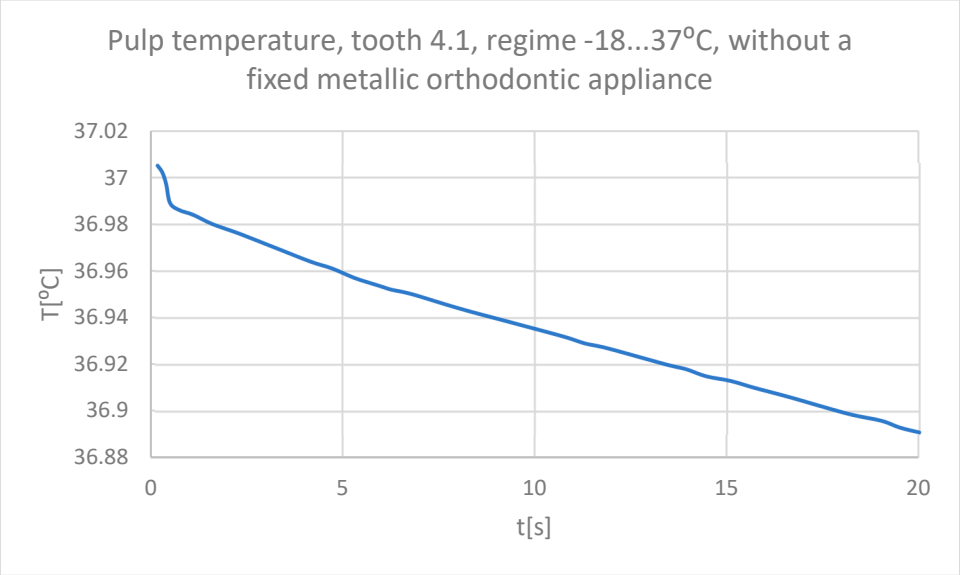

Figure 42. The temperature in the pulp of tooth 4.1 subjected to the cold thermal source.

Preprints.org (www.preprints.org) | NOT PEER-REVIEWED | Posted: 11 September 2024 doi:10.20944/preprints202409.0865.v1

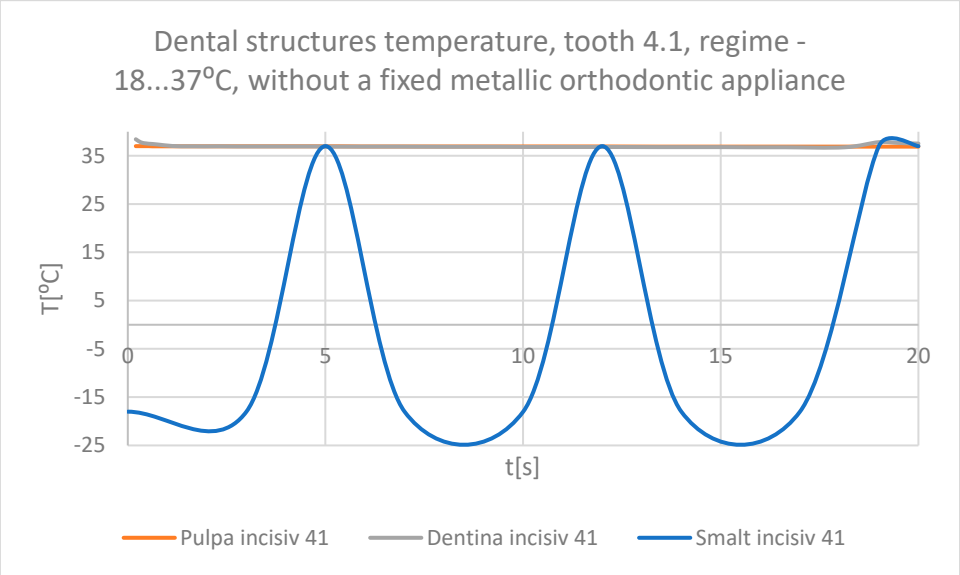

Figure 43. Comparative diagram of the dental structures temperatures of tooth 4.1 subjected to the cold thermal source.

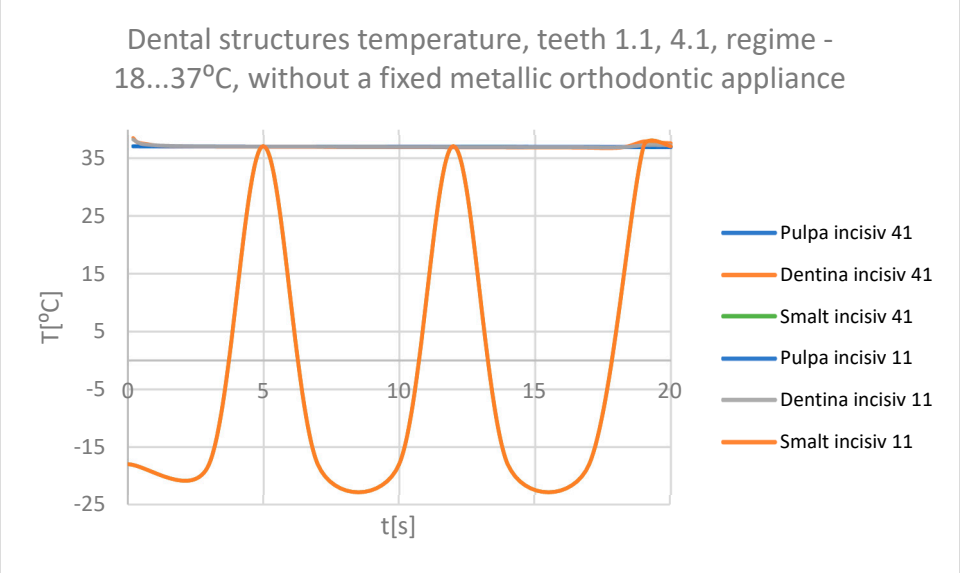

Figure 44. Comparative diagram of the dental structures temperatures of teeth 1.1, 4.1 subjected to the cold thermal source.

3.3. The Results of the Thermal Simulation for the Stomatognathic System with a Fixed Metallic Orthodontic Appliance Having a Hot Temperature Source

Figure 45 shows the temperature map of the system subjected to thermal simulation.

 doi:10.20944/preprints202409.0865.v1

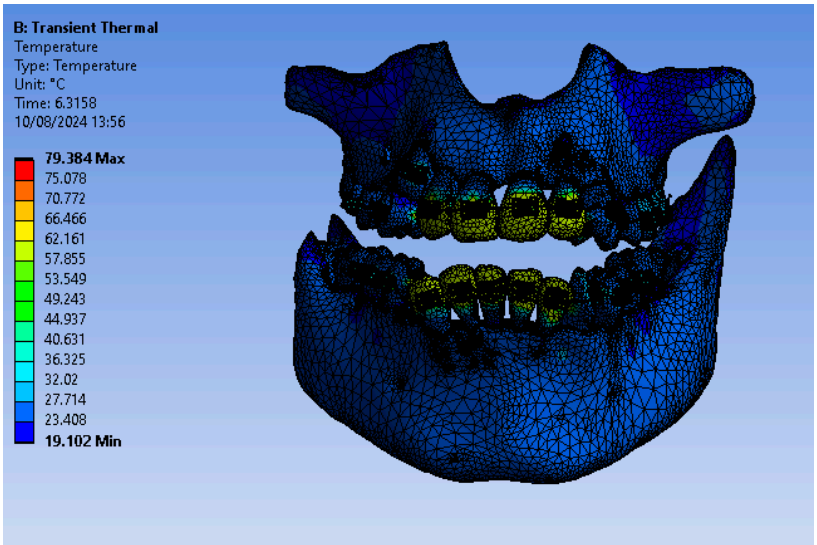

Figure 45. Temperature map.

Using the Probe-type virtual temperature sensors, the temperature diagram of the dental enamel (Figure 46), of the dentine (Figure 47), of the pulp (Figure 48) was obtained for tooth 1.1, the comparative diagram of the dental structures was obtained for tooth 1.1 (Figure 49), the temperature diagram of the dental enamel (Figure 50), of the dentine (Figure 51), of the pulp (Figure 52) was obtained for tooth 4.1, the comparative diagram of the dental structures was obtained for tooth 4.1 (Figure 53) and the comparative diagram of the dental structures was obtained for teeth 1.1, 4.1 (Figure 54).

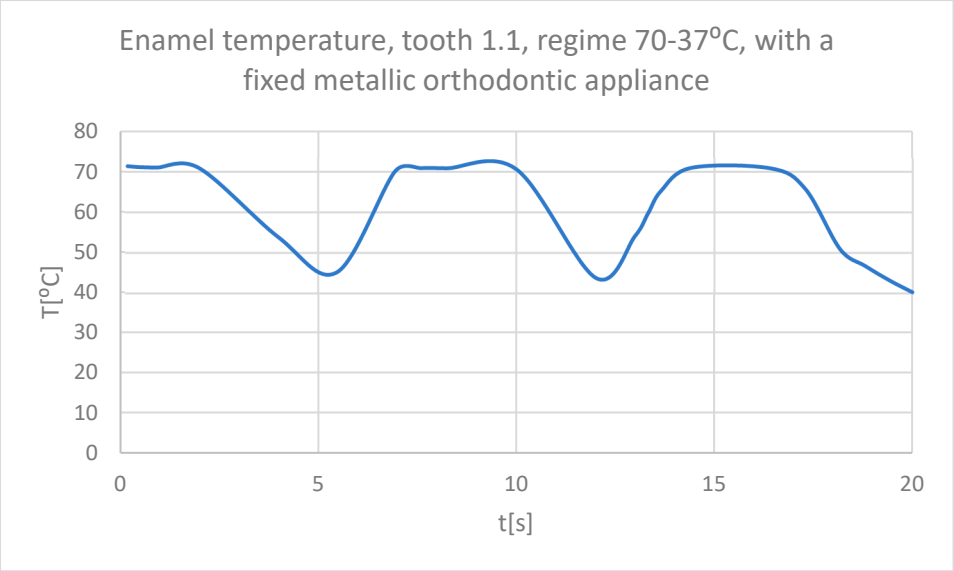

Figure 46. The temperature in the dental enamel of tooth 1.1 subjected to the hot thermal source.

 doi:10.20944/preprints202409.0865.v1

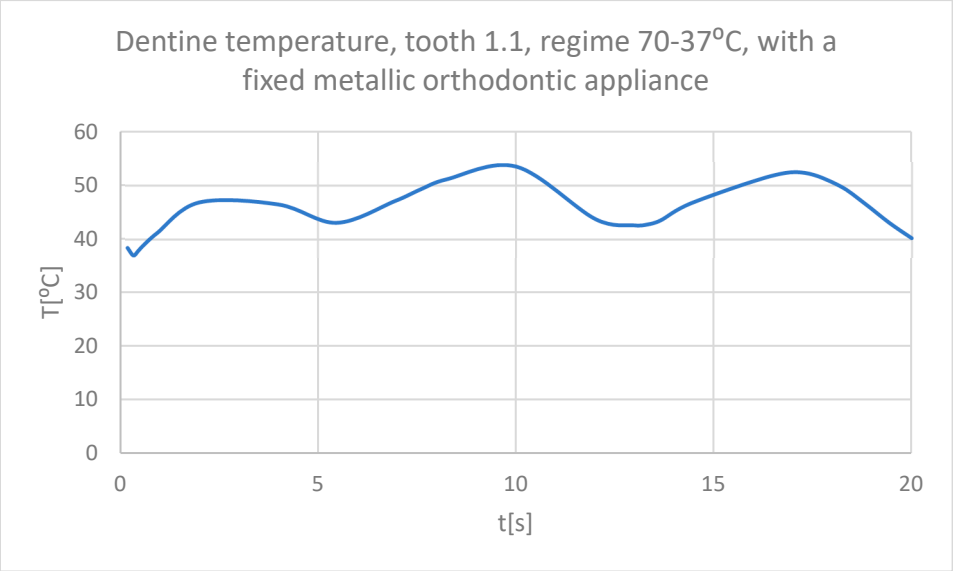

Figure 47. The temperature in the dentine of tooth 1.1 subjected to the hot thermal source.

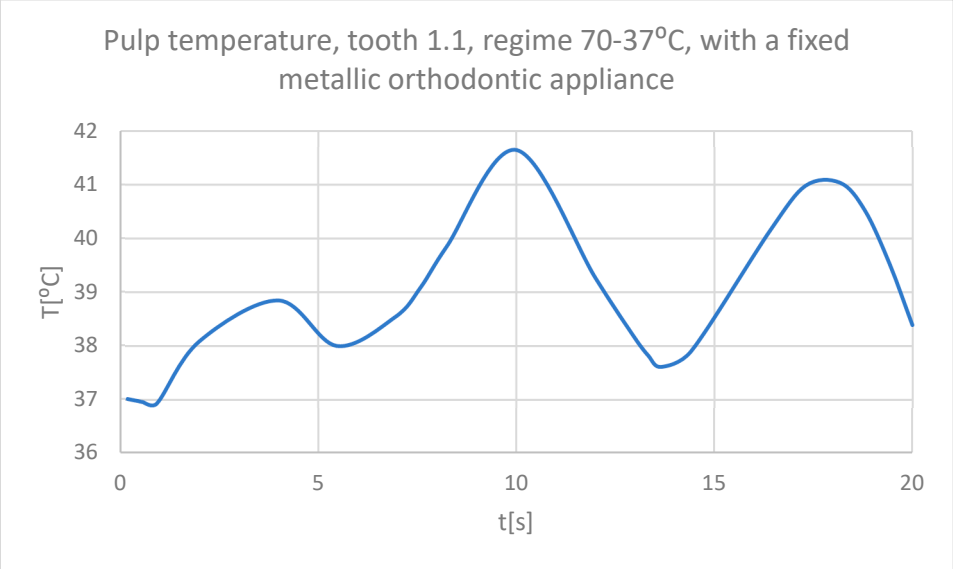

Figure 48. The temperature in the pulp of tooth 1.1 subjected to the hot thermal source.

 doi:10.20944/preprints202409.0865.v1

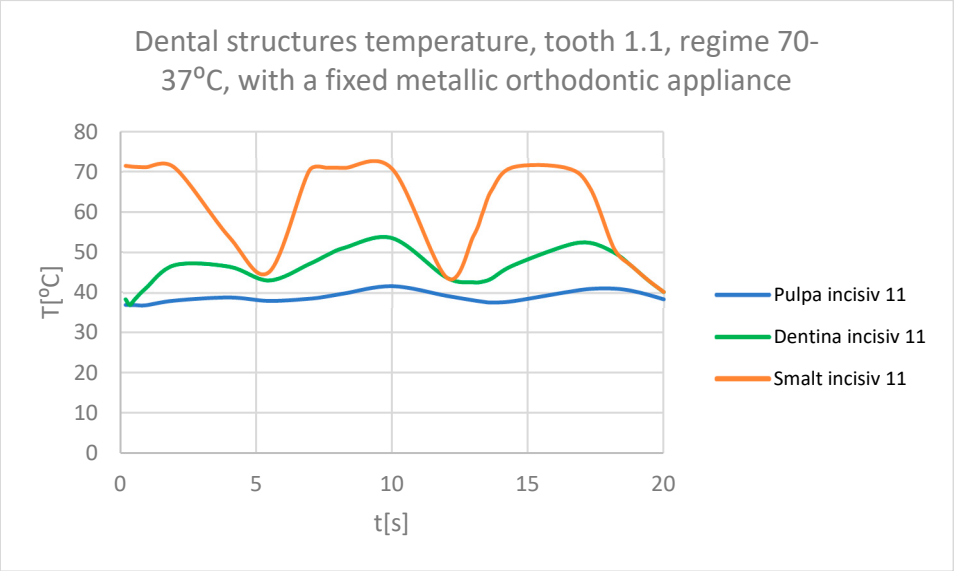

Figure 49. Comparative diagram of the dental structures temperature of tooth 1.1 subjected to the hot thermal source.

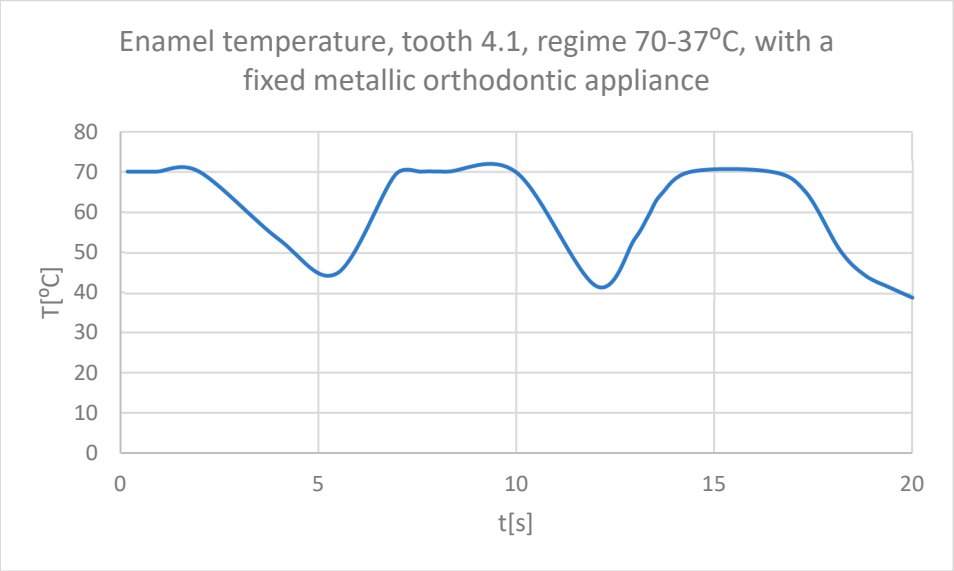

Figure 50. The temperature in the dental enamel of tooth 4.1 subjected to the hot thermal source.

 doi:10.20944/preprints202409.0865.v1

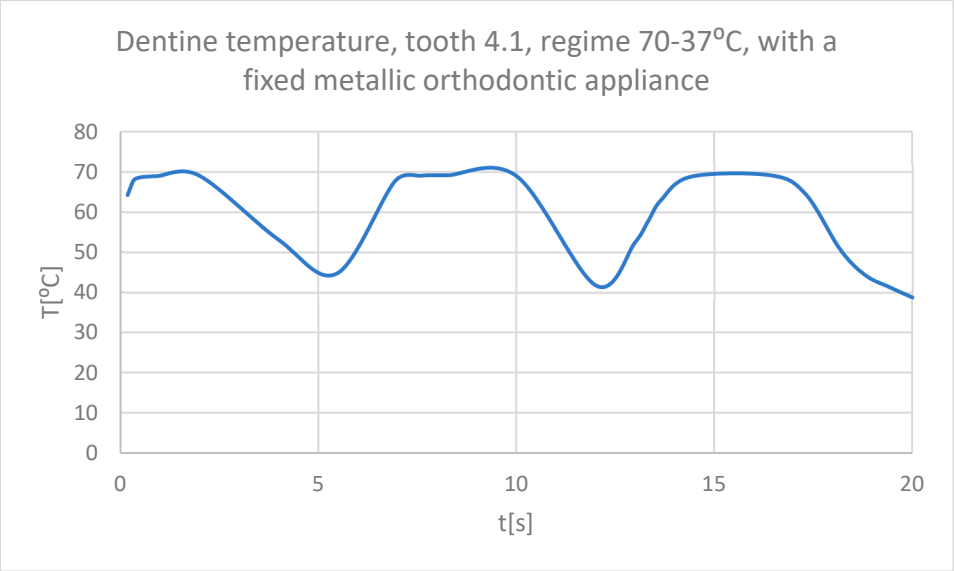

Figure 51. The temperature in the dentin of tooth 4.1 subjected to the hot thermal source.

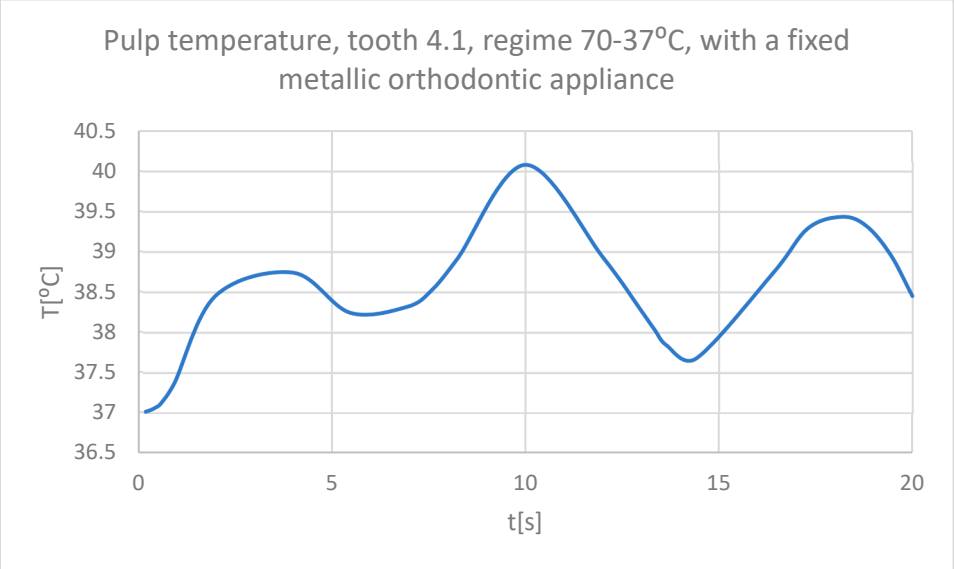

Figure 52. The temperature in the pulp of tooth 4.1 subjected to the hot thermal source.

Preprints.org (www.preprints.org) | NOT PEER-REVIEWED | Posted: 11 September 2024 doi:10.20944/preprints202409.0865.v1

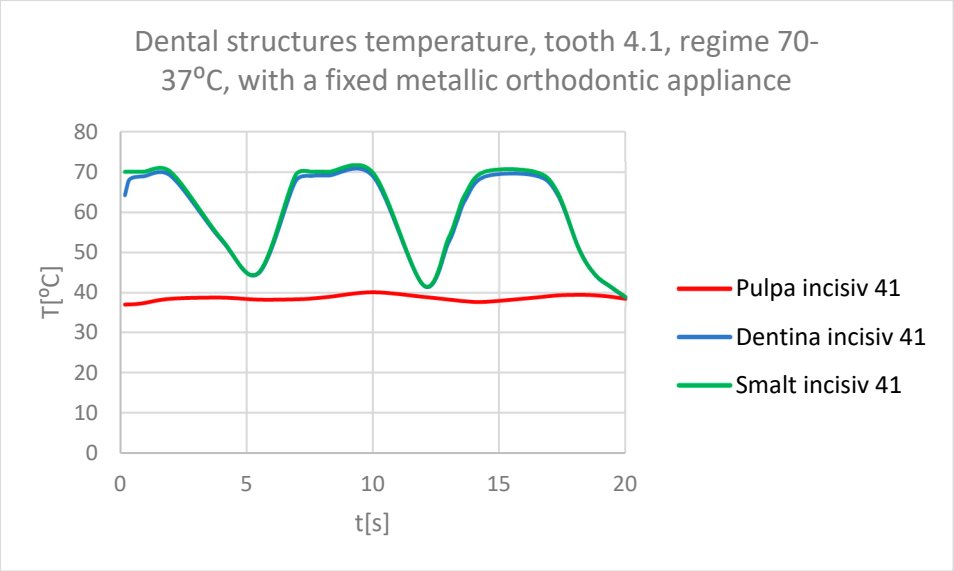

Figure 53. Comparative diagram of the dental structures temperature of tooth 4.1 subjected to the hot thermal source.

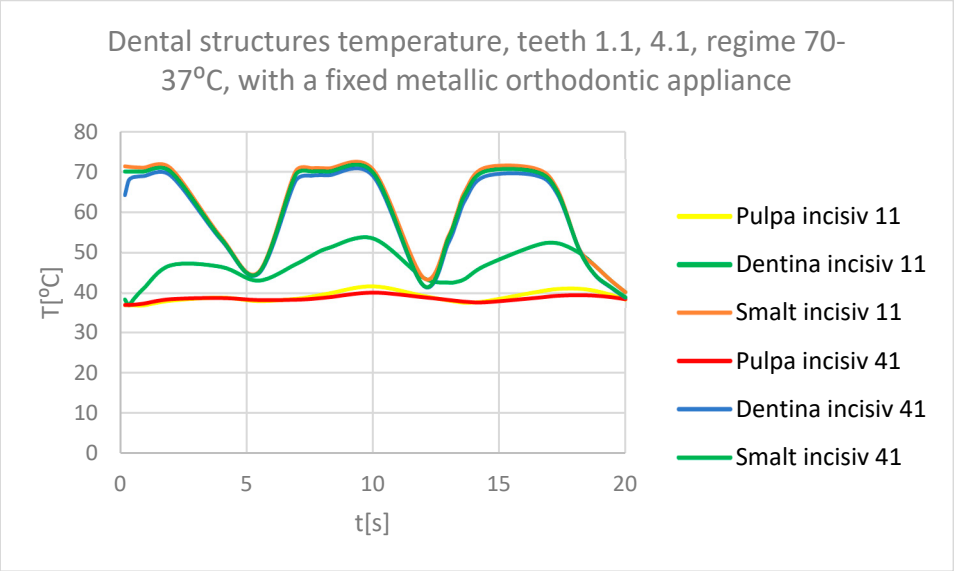

Figure 54. Comparative diagram of the dental structures temperature of teeth 1.1, 4.1 subjected to the hot thermal source.

3.4. Thermal Simulation Results for the Stomatognathic System with a Fixed Metallic Orthodontic Appliance, Having a Cold Temperature Source

Figure 55 shows the temperature map of the system subjected to thermal simulation.

Preprints.org (www.preprints.org) | NOT PEER-REVIEWED | Posted: 11 September 2024 doi:10.20944/preprints202409.0865.v1

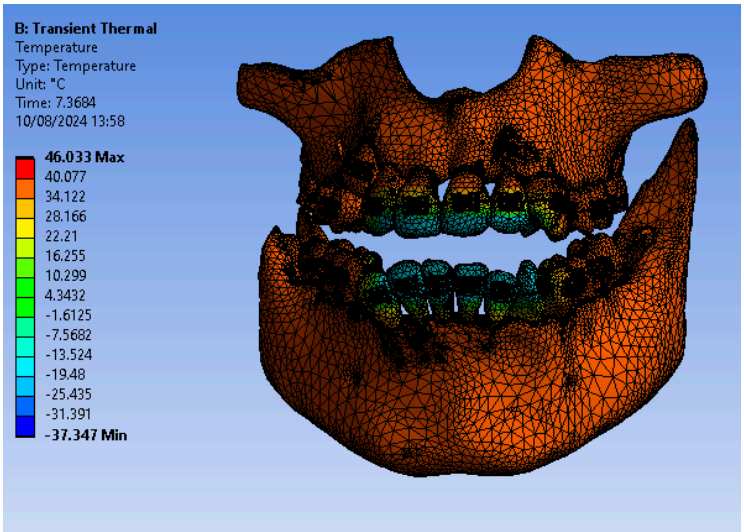

Figure 55. Temperature map.

Using the Probe-type virtual temperature sensors, the temperature diagram of the tooth enamel (Figure 56), of the dentine (Figure 57), of the pulp (Figure 58) was obtained for tooth 1.1, the comparative diagram of the dental structures was obtained for tooth 1.1 (Figure 59), the temperature diagram of the dental enamel (Figure 60), of the dentine (Figure 61), of the pulp (Figure 62) was obtained for tooth 4.1, the comparative diagram of the dental structures was obtained for tooth 4.1 (Figure 63) and the comparative diagram of the dental structures was obtained for teeth 1.1, 4.1 (Figure 64).

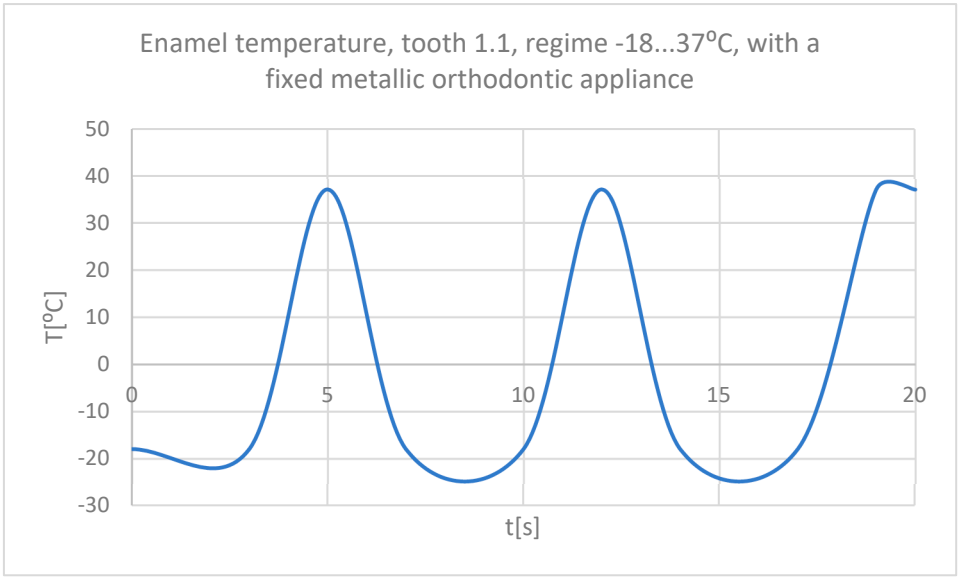

Figure 56. The temperature in the dental enamel of tooth 1.1 subjected to the cold thermal source.

 doi:10.20944/preprints202409.0865.v1

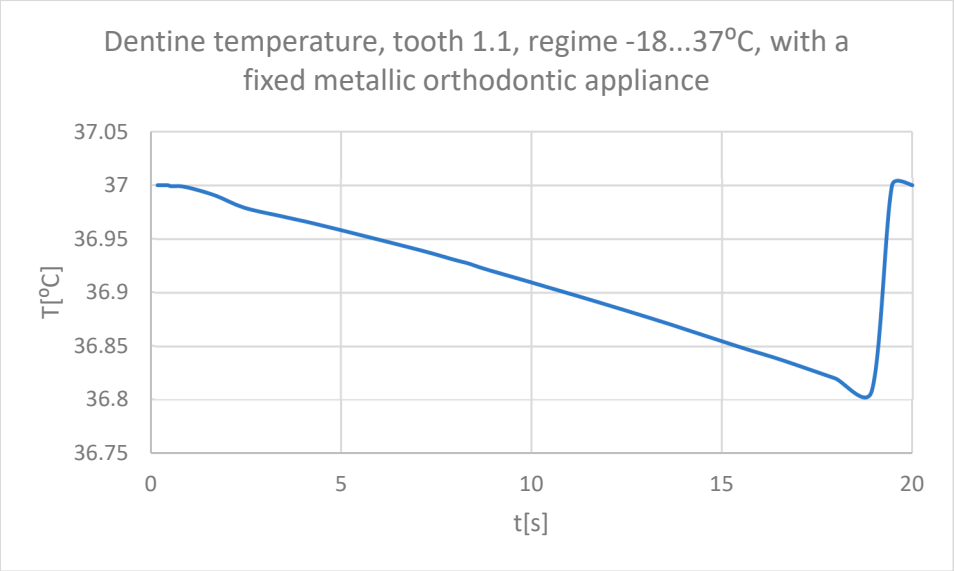

Figure 57. The temperature in the dentine of tooth 1.1 subjected to the cold thermal source.

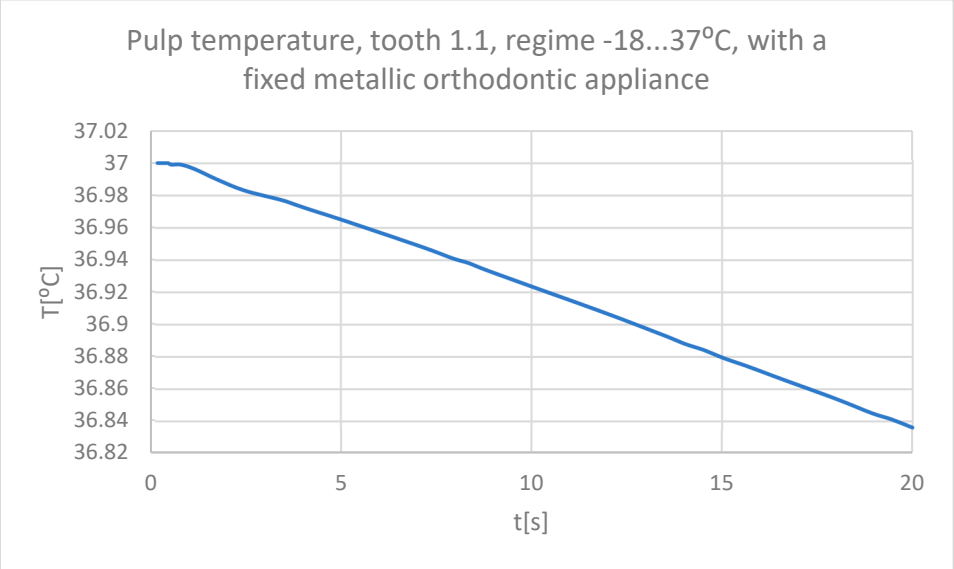

Figure 58. The temperature in the pulp of tooth 1.1 subjected to the cold thermal source.

 doi:10.20944/preprints202409.0865.v1

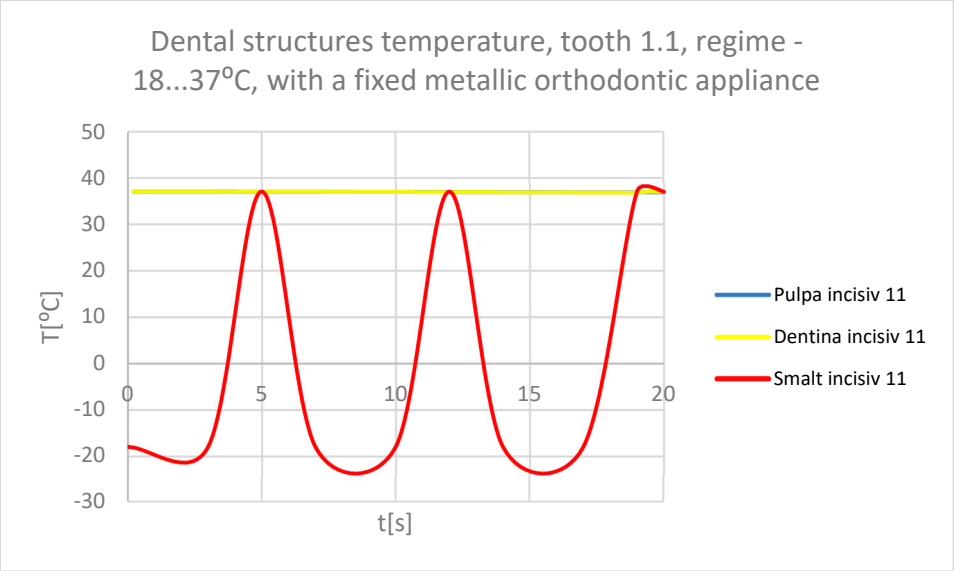

Figure 59. Comparative diagram of the dental structures temperature of tooth 1.1 subjected to the cold thermal source.

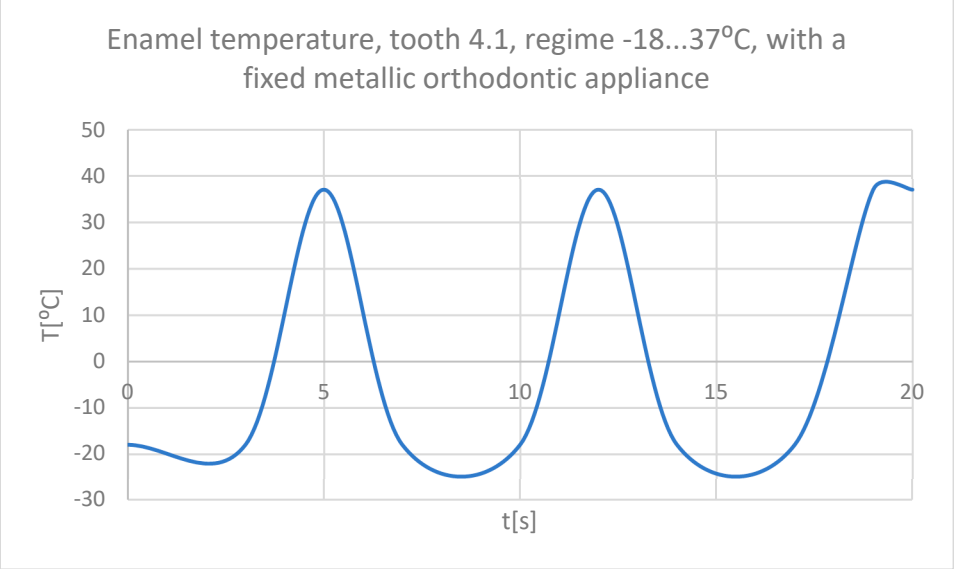

Figure 60. The temperature in the dental enamel of tooth 4.1 subjected to the cold thermal source.

 doi:10.20944/preprints202409.0865.v1

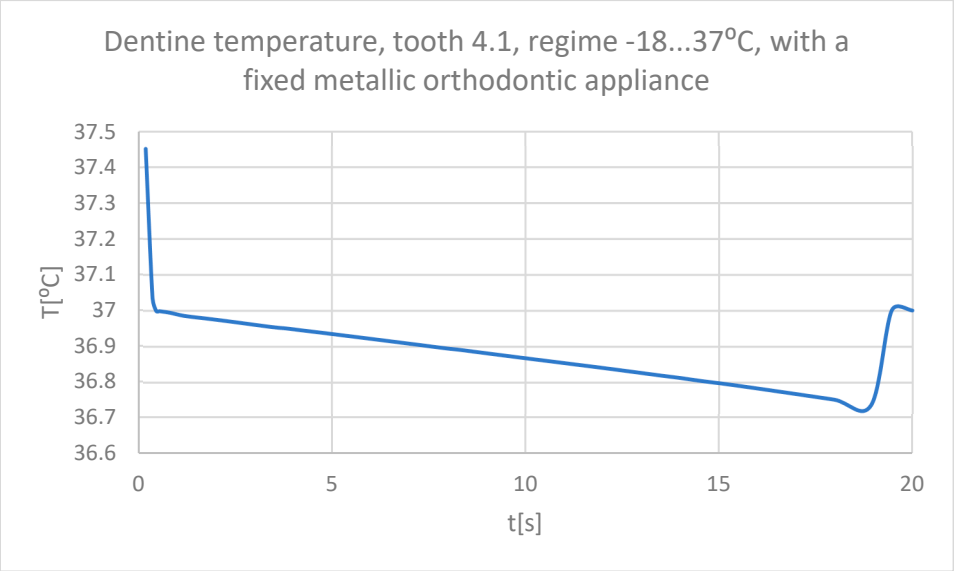

Figure 61. The temperature in the dentin of tooth 4.1 subjected to the cold thermal source.

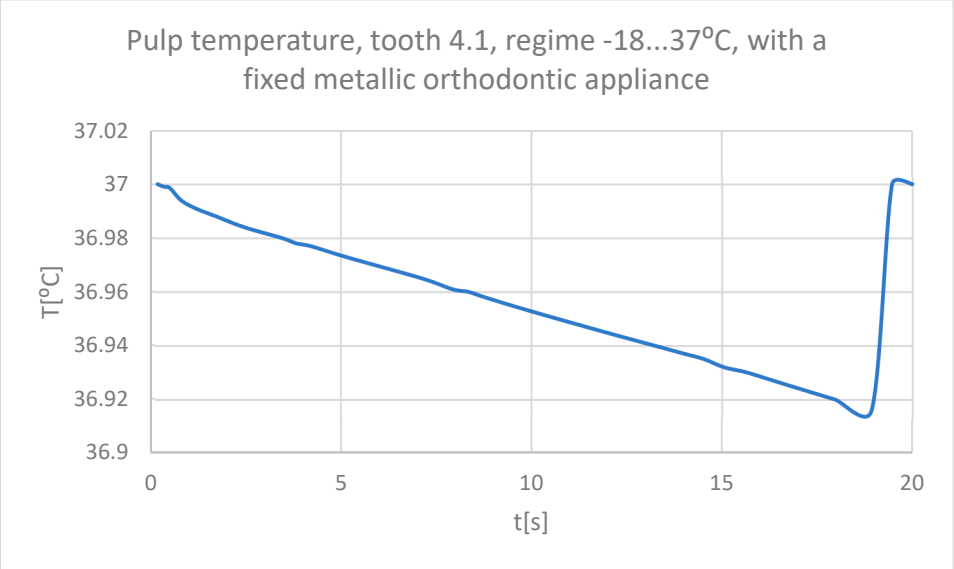

Figure 62. The temperature in the pulp of tooth 4.1 subjected to the cold thermal source.

Preprints.org (www.preprints.org) | NOT PEER-REVIEWED | Posted: 11 September 2024 doi:10.20944/preprints202409.0865.v1

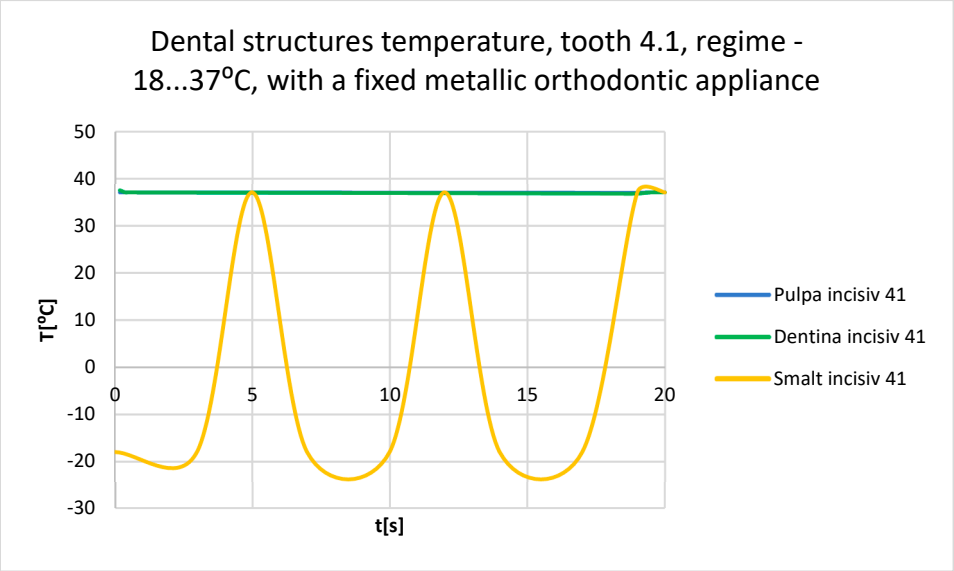

Figure 63. Comparative diagram of the dental structures temperature of tooth 4.1 subjected to the cold thermal source.

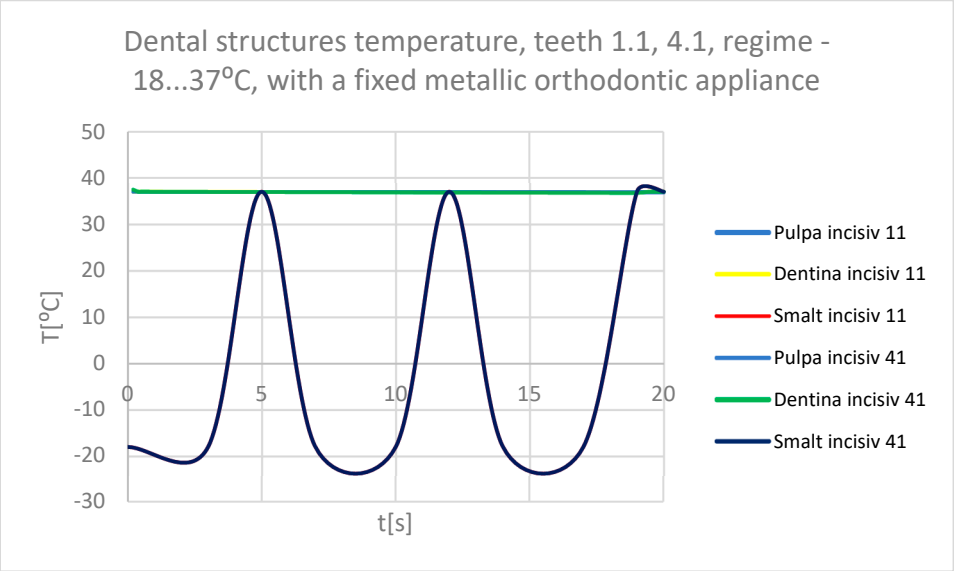

Figure 64. Comparative diagram of the dental structures temperature of teeth 1.1, 4.1 subjected to the cold thermal source.

3.5. Comparative Diagrams

It is known from the specialized literature that changing the temperature of the dental pulp by 5.5 ºC plus or minus can produce irreversible damage [18]. This finding assumes that, in the range of 31.5 ºC... 42.5 ºC, the dental pulp is intact and functional. In the following figures, Tmin=31.5 ºC and Tmax=42.5 ºC. Figure 65 shows a comparative diagram of the temperature effect on the dental pulp, with hot thermal source, for tooth 1.1.

Preprints.org (www.preprints.org) | NOT PEER-REVIEWED | Posted: 11 September 2024 doi:10.20944/preprints202409.0865.v1

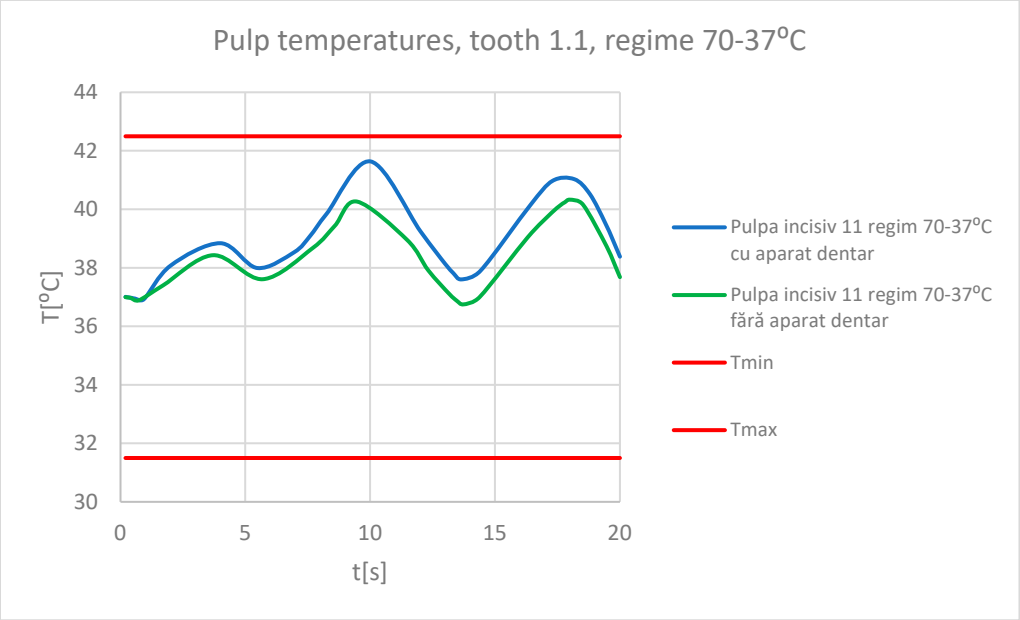

Figure 65. Comparative diagram of the temperature effect on the dental pulp, hot thermal source, for tooth 1.1.

Figure 66 shows a comparative diagram of the temperature effect on the dental pulp, hot thermal source, for tooth 4.1.

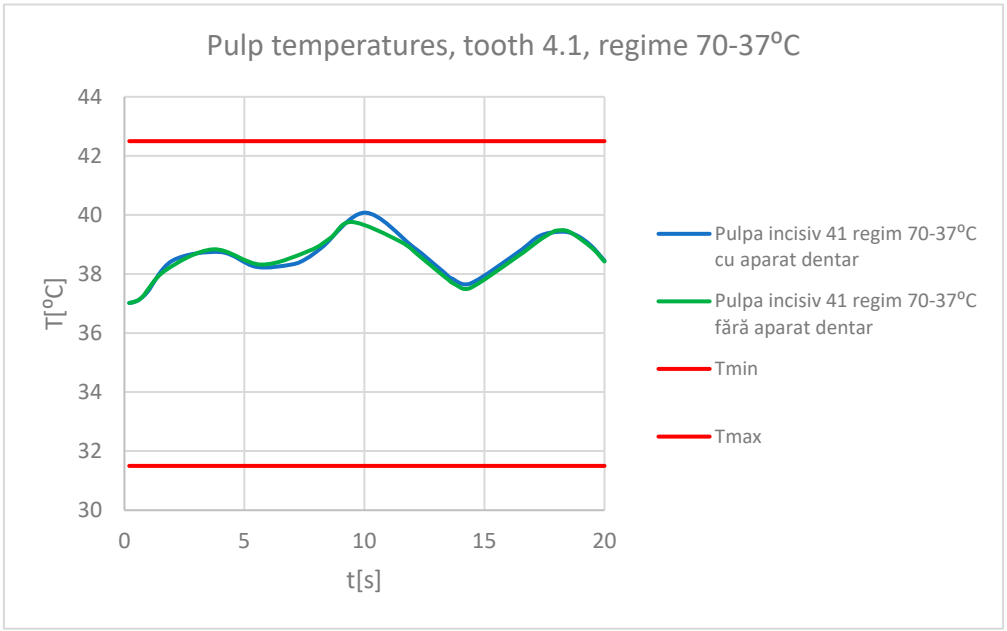

Figure 66. Comparative diagram of the temperature effect on the dental pulp, hot thermal source, for tooth 4.1.

Figure 67 shows a comparative diagram of the temperature effect on the dental pulp, cold thermal source, for tooth 1.1.

Preprints.org (www.preprints.org) | NOT PEER-REVIEWED | Posted: 11 September 2024 doi:10.20944/preprints202409.0865.v1

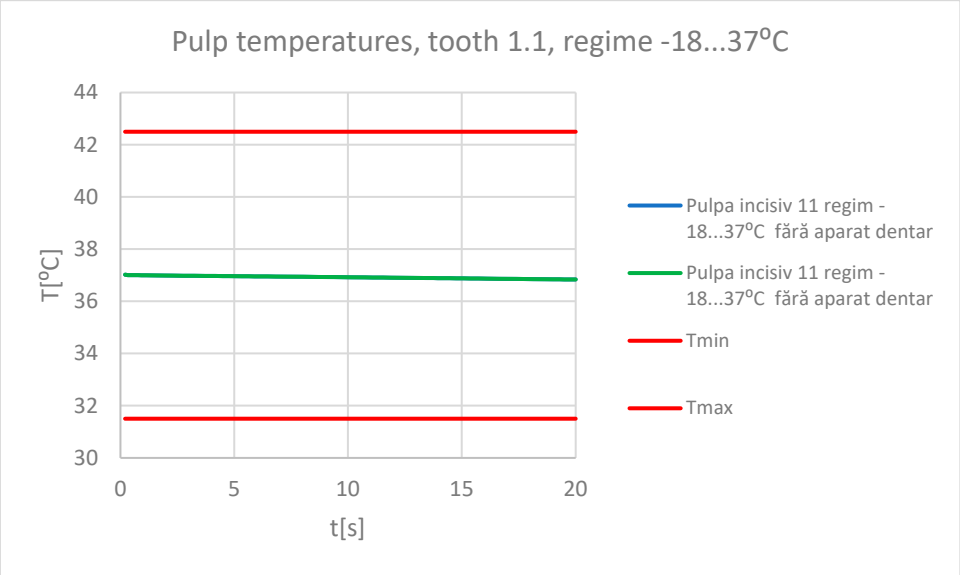

Figure 67. Comparative diagram of the temperature effect on the dental pulp, cold thermal source, for tooth 1.1.

Figure 68 shows a comparative diagram of the temperature effect on the dental pulp, cold thermal source, for tooth 4.1.

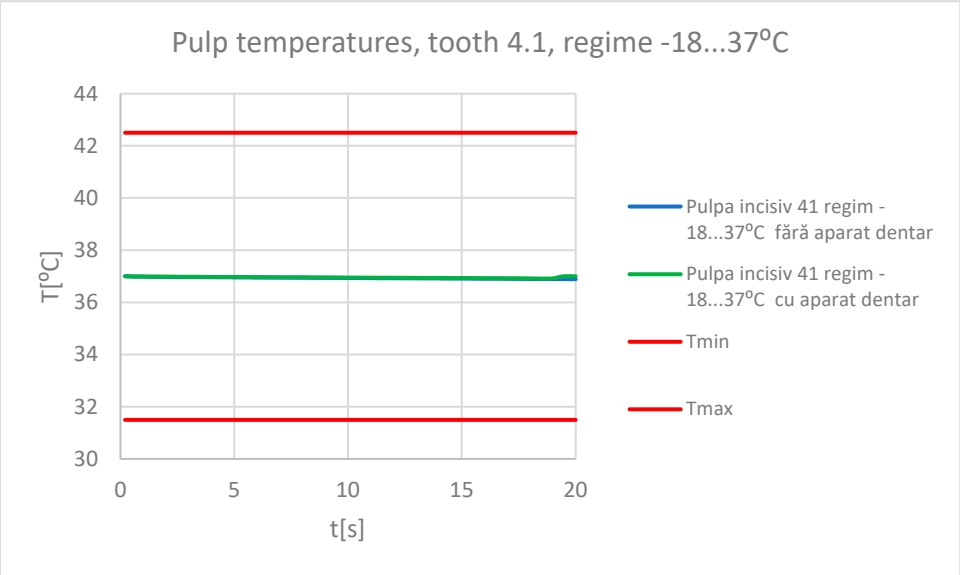

Figure 68. Comparative diagram of the temperature effect on the dental pulp, cold thermal source, for tooth 4.1.

Also, comparative diagrams were obtained for the two teeth for all thermal regimes, with or without a fixed metallic orthodontic appliance. Figure 69 shows the comparative diagram for the dental pulp of tooth 1.1 without a fixed metallic orthodontic appliance.

Preprints.org (www.preprints.org) | NOT PEER-REVIEWED | Posted: 11 September 2024 doi:10.20944/preprints202409.0865.v1

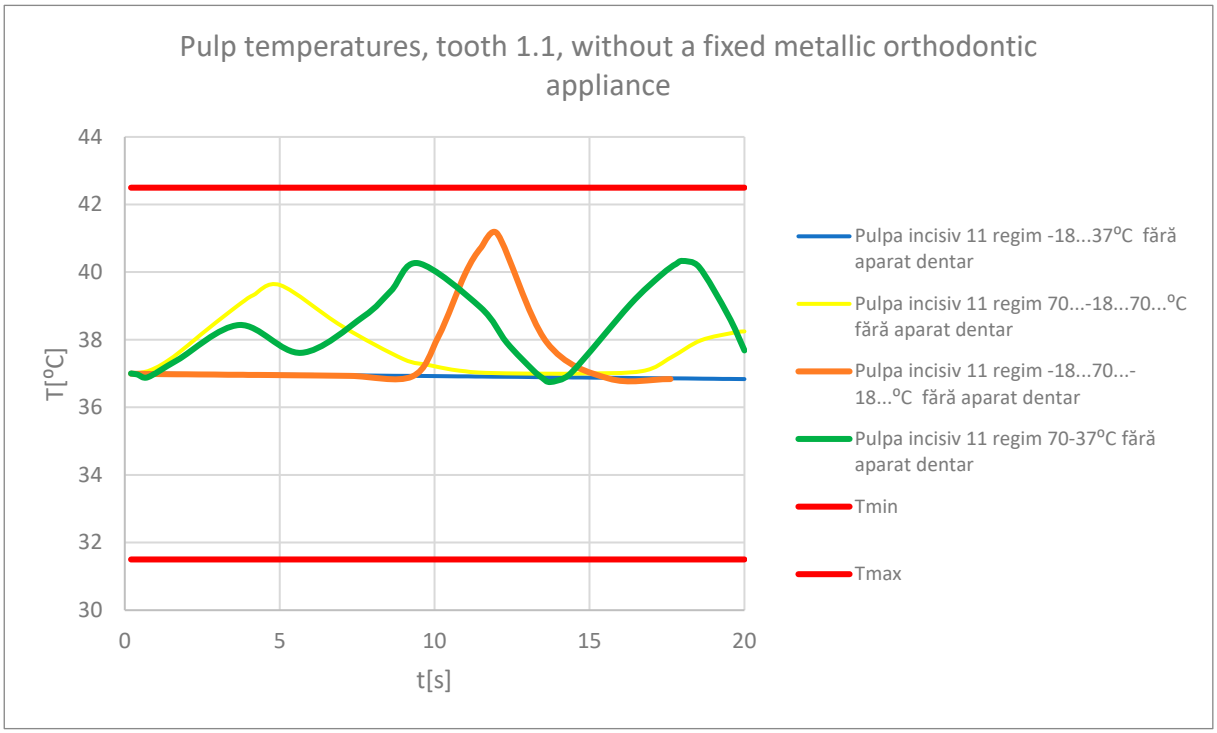

Figure 69. Comparative diagram for the dental pulp of tooth 1.1, without a fixed metallic orthodontic appliance.

Figure 70 shows the comparative diagram for the dental pulp of tooth 1.1, with a fixed metallic orthodontic appliance.

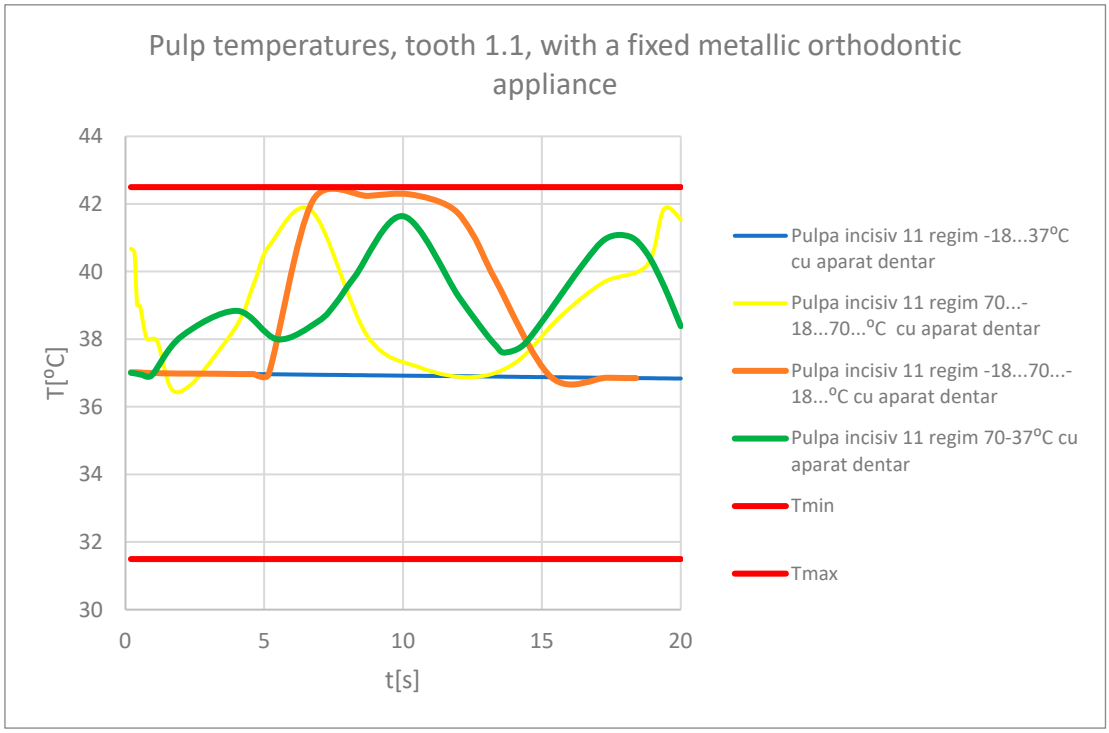

Figure 70. Comparative diagram for the dental pulp of tooth 1.1, with a fixed metallic orthodontic appliance.

Figure 71 shows the comparative diagram for the dental pulp of tooth 4.1, without a fixed metallic orthodontic appliance.

Preprints.org (www.preprints.org) | NOT PEER-REVIEWED | Posted: 11 September 2024 doi:10.20944/preprints202409.0865.v1

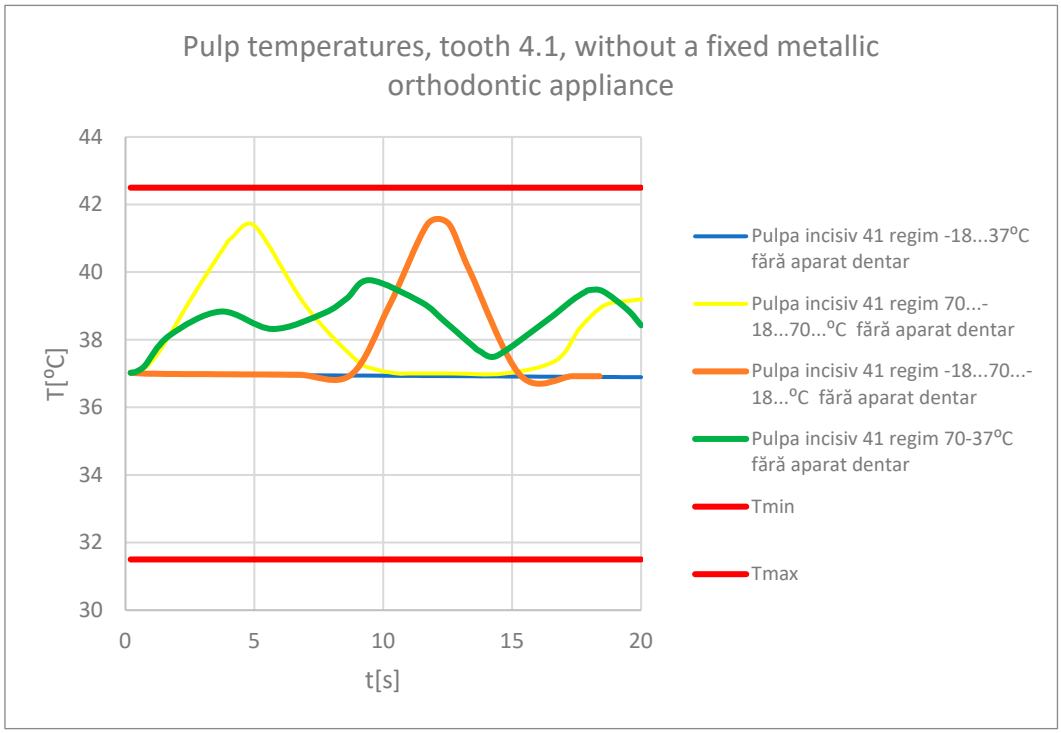

Figure 71. Comparative diagram for the pulp of tooth 4.1, without a fixed metallic orthodontic appliance.

Figure 72 shows the comparative diagram for the pulp of tooth 4.1, without a fixed metallic orthodontic appliance.

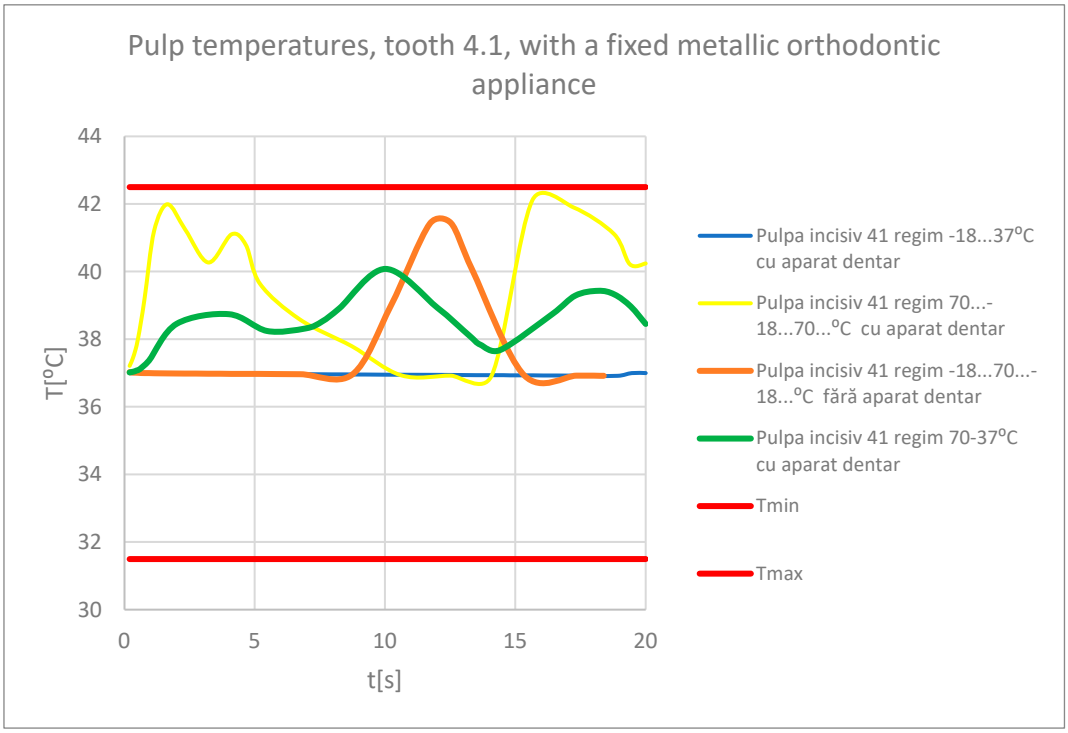

Figure 72. Comparative diagram for the pulp of tooth 4.1, with a fixed metallic orthodontic appliance.

 doi:10.20944/preprints202409.0865.v1

4. Discussion

In the specialized literature, there are few studies about thermal influence on different stomatognathic apparatus' structures using FEM.

In the early period of FEM application, many simulations did not directly lead to the expected results, but indirectly, they imposed important results in the field of materials testing or in the nonlinear analysis of force application in virtual human joints [19]. If initially, the analyzed models had a simplified geometry, and the division into finite elements was brief, nowadays, by improving the methods, multi-body structures with complicated loading configurations and complex constraints can be analyzed. Also, a series of physical phenomena have been interconnected and can be studied simultaneously, as simultaneous actions, such as thermal and structural study, and through the emergence of complex subroutines, rigid and flexible components with linear or non-linear mechanical behavior can be analyzed at the same time. In recent years, important progress has been made in the precise definition of the problem, but also in the multidisciplinary approach [20,21].

FEM can be utilized in the modeling and simulation of an orthodontic system, in order to determine the elastic forces that arise during orthodontic therapy with a fixed metallic appliance and the mechanical effect they cause. The study used CBCT scans from a patient who presented a malocclusion treated with the help of a fixed metallic orthodontic appliance. An upper orthodontic wire, a lower orthodontic wire, a set of bracket and tube-type elements were among the orthodontic components three-dimensional processed. A mathematical model of the forces that appear during fixed orthodontic treatment when a wire deforms was obtained using the Ansys Workbench program. As a result, the maximum deformation, maximum mechanical displacement, maximum stress, and deformation energy were determined [5].

FEM can also be used to determine the behavior of a real orthodontic system subjected to different systems of loads. To analyze the real orthodontic system, the researchers studied the case of patient with Angle class II malocclusion. With the help of InVesalius program, DICOM-type images obtained from CBCT scans were transformed into three-dimensional structures. After editing, modifying, completing, and analyzing the three-dimensional structures with Geomagic software, the researchers obtained a three-dimensional model made up of perfectly closed surfaces, that can be transformed into virtual solids. This model was loaded into CAD programs. Bracket and tube-type elements, as well as orthodontic wires were added to the model. The complete geometrical model was exported to AnsysWorkbench program, which uses FEM. The researchers performed simulations for the forces from 0.5 to 1 N. After these simulations, result maps were obtained, that showed the displacement, strain, and stress. After the study, the researchers found that, in addition to the known rigidity, the orthodontic system has elasticity due to the orthodontic wires and periodontal ligaments [6].

With varying degrees of periodontal tissue injury, a FEM study assessed the maximal stress, direction of force application, and displacement caused by the tooth-periodontal ligament-alveolar bone complex. The study showed that it is challenging to measure the forces produced during an orthodontic treatment with a fixed appliance from a clinical perspective. In the case of affected teeth, the researchers advise that the intensity of these forces should not exceed 1 N [22].

Another FEM study showed the biomechanical behaviour of fixed orthodontic retainers, especially the influence of their stiffness and tooth resilience on force transmission and stress distribution. Using FEM, the authors of the study obtained a virtual model of the lower jaw from canine to canine with a retainer attached on the oral surface of the six teeth. Applying axial or oblique loads on the central incisors, the force transmission increased from 2 to 65% with increasing tooth resilience and retainer stiffness. Also, the researchers concluded that a smaller retainer diameter reduced the uniformity of the stress distribution in the bonding interfaces, causing concentrated stress peaks within a small field of the bonding area. Thus, they recommend to avoid using fixed orthodontic retainers that are excessively stiff, especially on teeth with high resilience [23].

The limitations of our study are represented by the fact that we did not take into account the adhesive used for the bonding of the fixed metallic orthodontic appliance, which is found in a very thin layer between the base of the bracket or tube-type elements and the surface of the enamel. At the

 doi:10.20944/preprints202409.0865.v1

moment, the adhesives used in the field of orthodontics have thermal conductivity close to that of enamel, which is why we considered that it does not influence the results of our study.

In the future, we want to expand our research with similar FEM studies, alternating at short time intervals the thermal sources (cold-hot-cold and hot-cold-hot) to which various teeth are subjected.

5. Conclusions

FEM is an accurate method that can be used to generate three-dimensional virtual models of the stomatognathic apparatus and to simulate the influence of different thermal stimuli on tooth structures.

This study's findings indicate that any kind of FEM analysis can be performed beginning with a real patient's pre-treatment CBCT scans and virtual representations of the orthodontic wires, bracket and tube-type elements.

From the analysis of the obtained data, it was concluded that, following the simulations carried out in the presence of the fixed metallic orthodontic appliance, significantly higher temperatures were generated in the dental pulp. Therefore, the quality of the materials used to manufacture orthodontic adhesives, metallic bracket and tube-type elements can be increased with the help of FEM analyses.

Author Contributions: Conceptualization, S.-M.-S.P., M.P., G.B., A.M.R. and D.L.P.; methodology, S.-M.-S.P., M.R.P., D.D.V. and A.D.; validation, M.R.P., S.-M.-S.P., M.P. and D.D.V.; resources, S.-M.-S.P., M.P., A.M.R., D.I. and L.D.R.; data curation, M.R.P., S.-M.-S.P., M.P., G.B. and D.L.P.; writing-original draft preparation, S.-M.-S.P., M.P., A.D., D.I. and D.D.V.; writing-review and editing, M.R.P., D.L.P., D.I. and D.D.V.; visualization, S.-M.-S.P., M.P., A.M.R. and L.D.R.; supervision, M.R.P., D.L.P. and D.I.; project administration, S.-M.-S.P., M.P., D.L.P. and A.M.R. All authors have read and agreed to the published version of the manuscript.

Funding: Article publication charges were supported by the University of Craiova.

Institutional Review Board Statement: The study was conducted according to the guidelines of the Declaration of Helsinki and approved by the Ethics Committee of the University of Medicine and Pharmacy of Craiova (approval reference no. 127/09.04.2024).

Informed Consent Statement: Written informed consent was obtained from the subject involved in the study.

Data Availability Statement: The authors declare that the data from this research are available from the corresponding authors upon reasonable request.

Conflicts of Interest: The authors declare no conflict of interest.

References

1. Alhammadi, M.; Halboub, E.; Salah-Fayed, M.; Labib, A.; El-Saaidi, C. Global distribution of malocclusion traits: A systematic review. Dent. Press J. Orthod. 2018, 23, 40.e1–40.e10.
2. Petrescu, S.-M.-S.; Pisc, R.M.; Ioana, T.; Mărășescu, F.I.; Manolea, H.O.; Popescu, M.R.; Dragomir, L.P.; Dragomir, L.C.; Florea, Ș.; Bărăscu-Petrescu, R.A.; Ionescu, M.; Rauten, A.M. Prevalence of Malocclusions among Schoolchildren from Southwestern Romania. Diagnostics. 2024, 14, 705.
3. Friedlander-Barenboim, S.; Hamed, W.; Zini, A.; Yarom, N.; Abramovitz, I.; Chweidan, H.; Finkelstein, T.; Almoznino, G. Patterns of Cone-Beam Computed Tomography (CBCT) Utilization by Various Dental Specialties: A 4-Year Retrospective Analysis from a Dental and Maxillofacial Specialty Center. Healthcare. 2021, 9, 1042.
4. Jain, S.; Khoudhary, K.; Nagi, R.; Shukla, S.; Kaur, N.; Grover, D. New evolution of cone-beam computed tomography in dentistry: Combining digital technologies. Imaging Sci. Dent. 2019, 49, 179-190.
5. Petrescu, S.-M.-S.; Țuculină, M.J.; Popa, D.L.; Duță, A.; Sălan, A.I.; Voinea-Georgecu, R.; Diaconu, O.A.; Turcu, A.A.; Mocanu, H.; Nicola, A.G.; Dascălu, I.T. Modeling and Simulating an Orthodontic System Using Virtual Methods. Diagnostics. 2022, 12, 1296.
6. Katta, M.; Petrescu, S.-M.-S.; Dragomir, L.P.; Popescu, M.R.; Voinea-Georgescu, R.; Țuculină, M.J.; Popa, D.L.; Duță, A.; Diaconu,O.A.; Dascalu, I.T. Using the Finite Element Method to Determine the Odonto-Periodontal Stress for a Patient with Angle Class II Division 1 Malocclusion. Diagnostics. 2023, 13, 1567.
7. Tarniță, D.; Boborelu, C.; Popa, D.L.; Tarniță, C.; Rusu, L. The three-dimensional modeling of the complex virtual human elbow joint. Rom. J. Morphol. Embryol. 2010, 51, 489-495.
8. Zach, L.; Cohen, G. Pulp response to external heat. Oral Surg. 1965, 19, 515-530.

9. Korioth, T.W.; Versluis, A. Modeling the mechanical behavior of the jaws and their related structures by finite element (FE) analysis. Crit. Rev. Oral Biol. Med. 1997, 8, 90-104.
10. Rees, J.S.; Jacobsen, P.H. The effect of cuspal flexure on a buccal Class V restoration: A finite element study. J. Dent. 1998, 26, 361-367.
11. Toparli, M.; Gökay, N.; Aksoy, T. An investigation of temperature and stress distribution on a restored maxillary second premolar tooth using a three-dimensional finite element method. J. Oral Rehabil. 2000, 27, 1077-1081.
12. Masouras, K.; Silikas, N.; Watts, D.C. Correlation of filler content and elastic properties of resin-composites. Dent. Mater. 2008, 24, 932-939.
13. Nica, I.; Rusu, V.; Păun, A.; Ștefănescu, C.; Vizureanu, P.; Alugulesei, A. Thermal properties of nanofilled and microfilled restorative composites. Mater. Plast. 2009, 18, 20.
14. Hashemipour, M.A.; Mohammadpour, A.; Nassab, S.A. Transient thermal and stress analysis of maxillary second premolar tooth using an exact three-dimensional model. Indian J. Dent. Res. 2010, 21, 158-164.
15. Ausiello, P.; Franciosa, P.; Martorelli, M.; Watts, D.C. Numerical fatigue 3D-FE modeling of indirect composite-restored posterior teeth. Dent. Mater. 2011, 27, 423-430.
16. Alnazzawi, A.; Watts, D.C. Simultaneous determination of polymerization shrinkage, exotherm and thermal expansion coefficient for dental resin-composites. Dent. Mater. 2012, 28, 1240-1249.
17. Xie, H.; Deng, S.; Zhang, Y.; Zhang, J. Simulation study on convective heat transfer of the tongue in closed mouth. 8th IEEE International Conference on Software Engineering and Service Science (ICSESS). 2017, 802-805.
18. Stănuşi, A.Ş.; Popa, D.L.; Ionescu, M.; Cumpătă, C.N.; Petrescu, G.S..; Ţuculină, M.J.; Dăguci, C.; Diaconu, O.A.; Gheorghiță, L.M.; Stănuşi, A. Analysis of Temperatures Generated During Conventional Laser Irradiation of Root Canals–A Finite Element Study. Diagnostics. 2023, 13, 1757.
19. Huiskes, R.; Chao, E.Y.S. A Survey of Finite Element Analysis in Orthopedic Biomechanics: The First Decade. J. Biomech. 1983, 16, 385–409.
20. Shivakumar, S.; Kudagi, V.S.; Talwade, P. Applications of Finite Element Analysis in Dentistry: A Review. J. Int. Oral Health. 2021, 13, 415-422.
21. Rastegari, S.; Hosseini, S. M.; Hasani, M.; Jamilian, A. An Overview of Basic Concepts of Finite Element Analysis and Its Applications in Orthodontics. J. Dentists. 2023, 11, 23–30.
22. Luchian, I.; Mârțu, M.A.; Tatarciuc, M.; Scutariu, M.M.; Ioanid, N.; Pasarin, L.; Kappenberg-Nițescu, D.C.; Sioustis, I.A.; Solomon, S.M. Using FEM to Assess the Effect of Orthodontic Forces on Affected Periodontium. Appl. Sci. 2021, 11, 7183.
23. Hetzler, S.; Rues, S.; Zenthöfer, A.; Rammelsberg, P.; Lux, C.J.; Roser, C.J. Finite Element Analysis of Fixed Orthodontic Retainers. Bioengineering. 2024, 11, 394.